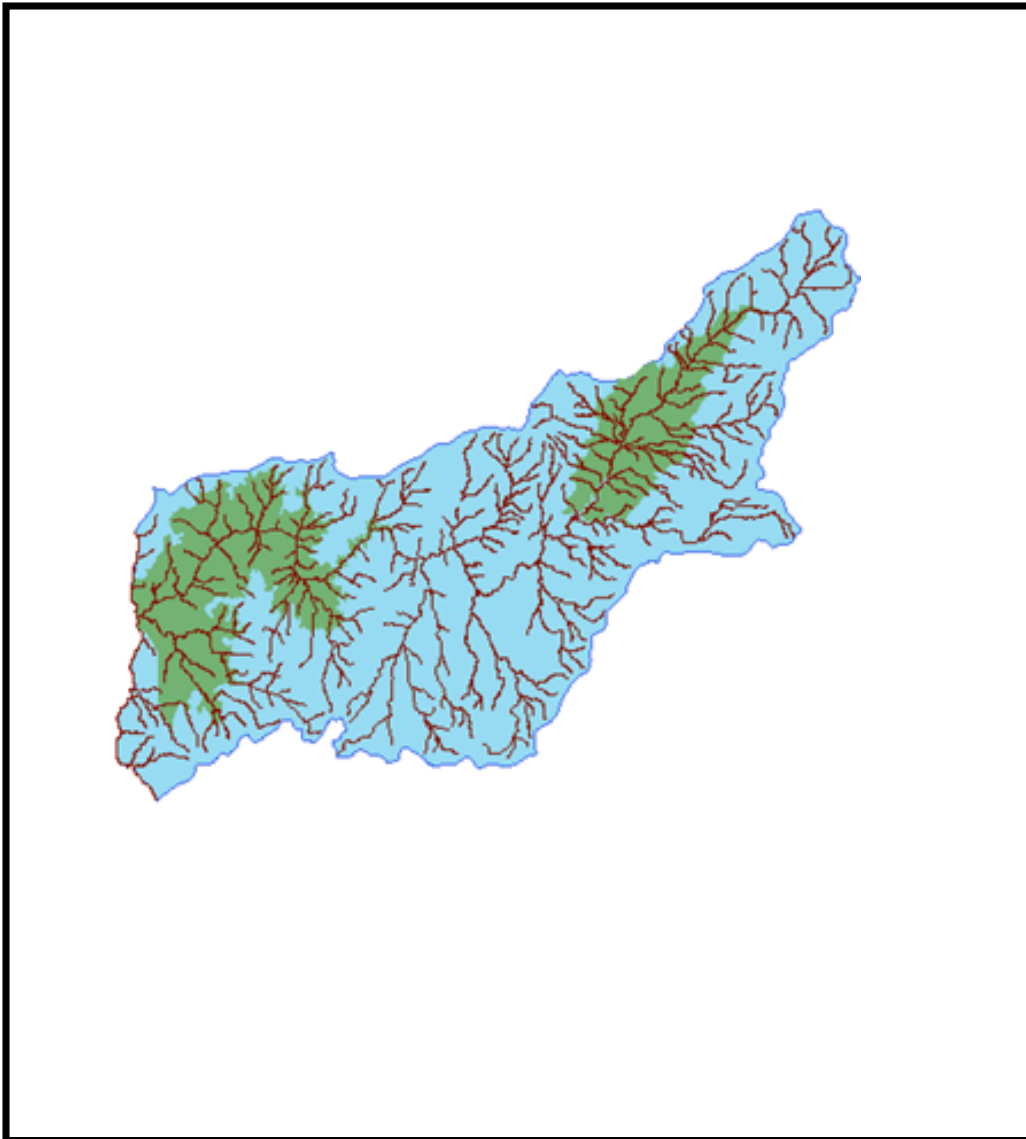


# UNESCO-IHE INSTITUTE FOR WATER EDUCATION



## **Hydrological Response of a Catchment to Climate Change, Case Study on Upper Beles Sub- Basin, Upper Blue Nile, Ethiopia**

**Girma Yimer Ebrahim**

MSc Thesis WSE-HI.08-16  
April 2008

UNESCO-IHE  
Institute for Water Education







UNESCO-IHE  
Institute for Water Education



## **Hydrological Response of a Catchment to Climate Change, Case Study on Upper Beles Sub- Basin, Upper Blue Nile, Ethiopia**

Master of Science Research  
by  
**Girma Yimer Ebrahim**

Supervisors

**Prof. D. P. Solomatine PhD, MSc (UNESCO-IHE)**  
**A. Jonoski, PhD, MSc (UNESCO-IHE)**  
**A.B.K. Van Griensven, PhD, MSc (UNESCO-IHE)**

Examination committee

**Prof. R. k. Price, PhD (UNESCO-IHE), Chairman**  
**Y. A. Mohamed, PhD, MSc (UNESCO-IHE, IWMI)**  
**A. Jonoski, PhD, MSc (UNESCO-IHE)**  
**A. B. K. Van Griensven, PhD, MSc (UNESCO-IHE)**

This research is done for the partial fulfillment of the requirements of the Master of Science degree at UNESCO-IHE Institute for Water Education, Delft the Netherlands

**Delft**  
**April 2008**

The findings, interpretations and conclusions expressed in this study do neither necessary reflect the views of the UNECSO-IHE Institute for Water Education, nor of the individual members of the MSC committee, nor of their respective employers.

## **Abstract**

Global warming will likely alter the hydrological cycle in a ways that have substantial impacts on water resource availability. Changes in temperature, precipitation amount, patterns and intensities and evapotranspiration will almost directly affect the water balance of the drainage basin and stream flow in rivers. Such changes in the hydrological cycle component will have significant impact on the local and regional hydrological regimes which in turn affects ecological, social and economical systems.

Although quantitative estimates of hydrologic effects of climate change are essential for understanding and solving the potential water resource management problems associated with power generation, agriculture and water resource planning and management, the current coarse resolution of general circulation models (GCMs) does not provide reliable estimates of meteorological variables at the appropriate scale required for regional impact assessments.

Hence more reliable meteorological variables such as temperature and rainfall corresponding to future climate scenarios can be derived from GCMs outputs using the so called 'downscaling techniques'. In this study Statistical downscaling model (SDSM) and Temporal Neural network were used to downscale the GCM model outputs in particular precipitation and temperature to generate the possible future scenarios in the Upper Beles Sub-Basin, Upper Blue Nile, Ethiopia. The downscaled meteorological variables were subsequently used as input to the HEC-HMS hydrological model to simulate the corresponding stream flow change.

Results of the impact assessment over the basin showed projected increase in annual runoff ranged from 18 % in 2050s to 11% in 2090s for A2a emission scenario. The Sensitivity analysis based on incremental scenarios showed that a drier and warmer climate change results in reduced runoff. A 20 % decrease in rainfall coupled with a 2 °c increase in temperature would result in a 41 % decrease in annual runoff.

**Keywords:** Upper Beles; Climate Change, SDSM, TLFN, HEC-HMS;



## **Acknowledgments**

Many people, more than can be mentioned, contributed in various ways to the completion of this study to all of whom I am most grateful. I apologize if any one feels that his/her name should have been mentioned.

First of all I would like to express my sincere gratitude to Dr. Andreja Jonoski, my main supervisor, for his guidance and insightful comments extended through out my research. I would like also to express my sincere gratitude to my mentor Dr. Ann VanGrensiven for her guidance, encouragements and moral support

I am extremely grateful to Dr. Yonas Berhan for his continuous support from the inception of this work to the end. I would like also to thank Dr. Yonas's friend Dr. Dimitri for providing me GCM data and other publications

I wish to express my sincere gratitude to all NBI staff: Dr. Hesham Ghany, Dr. Abdulikarim H. seid, Dr. Solomon Seyoum, Dr. Mekureya Beyene, Ato Dekseyous Tarekegen, Ato Fisum, Ato zegeye for all their support and Advice. In particular I would like to thank Dr. Solomon Seyoum for his help in coding

I wish to express my heart felt thanks to Mr. Lijalem Zeray and Abdo kedir for their support and feedbacks I got from them

I am also grateful to Pawe Agricultural Research office and Pawe woreda Agricultural office for their support and facilitation during my field visit. I would like also to thank the Hydrology Department of MOWR and NMA of Ethiopia for providing me data free of charge

I would like to thank Mr. Gerald Corzo for his help In Mat lab script development. I would like to thank Mr. Ashenafi , Mr. Daneil , Dr. Ungtage Kim for their support

I would like to express my greatest gratitude to the NBI scholarship

My deepest gratitude goes to my fiancée Selamawit Assefa who endured multiple hardships during the course of this study. With out her persistent, encouragements and support my study would no have been made possible

I am very grateful to my brother Assfaw who is my source of confidence and who is the reason for who I am now. And I am also equally grateful to my parents

I would like to thank my best friends Sirak, Tizitaw, Maregu and Tessema for their encouragement, moral support and true friendship.

Last but not least I praise the Almighty GOD for his love and blessings all along my ways

Girma Yimer Ebrahim





## Table of content

|  |           |
|--|-----------|
| ABSTRACT .....   | I         |
| ACKNOWLEDGMENTS .....  | III       |
| LIST OF SYMBOLS /ACRONYMS .....                                    | VII       |
| LISTS OF FIGURES .....   | IX        |
| LIST OF TABLES .....   | XI        |
| <b>1 INTRODUCTION.....</b>   | <b>1</b>  |
| 1.1 BACKGROUND.....  | 1         |
| 1.2 PROBLEM STATEMENT.....   | 2         |
| 1.3 RESEARCH OBJECTIVES.....                                       | 2         |
| 1.4 STRUCTURE OF THE THESIS.....                                   | 3         |
| <b>2 DESCRIPTION OF THE STUDY AREA.....</b>                        | <b>5</b>  |
| 2.1 TOPOGRAPHY .....   | 7         |
| 2.2 CLIMATE .....  | 7         |
| 2.3 LAND USE.....  | 7         |
| 2.4 SOIL .....   | 9         |
| 2.5 DRAINAGE NETWORKS.....   | 9         |
| 2.6 TANA BELES PROJECT .....                                       | 9         |
| <b>3 LITERATURE REVIEW.....</b>                                    | <b>15</b> |
| 3.1 GLOBAL CLIMATE CHANGE .....                                    | 15        |
| 3.2 CLIMATE MODELS.....  | 15        |
| 3.3 DOWNSCALING.....   | 16        |
| 3.3.1 <i>Dynamic downscaling</i> .....                             | 16        |
| 3.3.2 <i>Statistical downscaling</i> .....                         | 17        |
| 3.4 CLIMATE SCENARIOS.....   | 18        |
| 3.4.1 <i>Emissions Scenarios</i> .....                             | 19        |
| 3.5 KEY UNCERTAINTIES IN CLIMATE SCENARIOS.....                    | 21        |
| 3.6 CLIMATE CHANGE STUDIES ON BLUE NILE.....                       | 22        |
| <b>4 METHODOLOGY .....</b>   | <b>25</b> |
| 4.1 METEOROLOGICAL DATA.....                                       | 25        |
| 4.2 HYDROLOGICAL DATA.....   | 26        |
| 4.3 DATA SCREENING.....  | 26        |
| 4.4 WEATHER GENERATION .....                                       | 27        |
| 4.4.1 <i>ClimGen weather generator</i> .....                       | 28        |
| 4.4.2 <i>LARS-WG stochastic weather generator</i> .....            | 29        |
| 4.5 GENERAL CIRCULATION MODEL (GCM).....                           | 31        |
| 4.6 DOWNSCALING.....   | 32        |
| 4.6.1 <i>Statistical Downscaling Model (SDSM)</i> .....            | 32        |
| 4.6.2 <i>Artificial Neural Networks</i> .....                      | 36        |
| 4.7 HEC-HMS HYDROLOGICAL MODEL.....                                | 38        |
| 4.3.1 <i>Continuous soil moisture accounting (SMA) model</i> ..... | 38        |
| 4.3.2 <i>Clark Unit Hydrograph Transform</i> .....                 | 39        |
| 4.3.3 <i>Linear Reservoir Model</i> .....                          | 40        |
| 4.3.4 <i>Muskingum Model</i> .....                                 | 40        |
| 4.3.5 <i>HEC-HMS Model setup</i> .....                             | 40        |
| 4.3.6 <i>Basin Model</i> .....                                     | 41        |
| 4.3.7 <i>Meteorologic Model</i> .....                              | 42        |
| <b>5 RESULTS AND DISCUSSIONS .....</b>                             | <b>45</b> |
| 5.5 DATA ANALYSIS .....  | 45        |
| 5.1.1 <i>Data Screening</i> .....                                  | 45        |
| 5.1.2 <i>Weather generation</i> .....                              | 46        |
| 5.1.3 <i>Statistical tests</i> .....                               | 48        |
| 5.6 DOWNSCALING.....   | 50        |

|          |  |           |
|----------|--|-----------|
| 5.6.1    | <i>SDSM</i> .....  | 50        |
| 5.6.2    | <i>Time Lagged Feed forward Neural networks (TLFN)</i> .....                           | 57        |
| 5.7      | <b>HEC-HMS HYDROLOGICAL MODEL RESULTS</b> .....  | 61        |
| 5.7.1    | <i>Calibration</i> .....   | 61        |
| 5.7.2    | <i>Validation</i> .....  | 64        |
| 5.7.3    | <i>Model simulation corresponding to future climate change scenarios</i> .....         | 65        |
| 5.8      | <b>CROP WATER REQUIREMENTS</b> .....   | 67        |
| 5.9      | <b>SYNTHETIC SCENARIOS</b> .....   | 69        |
| <b>6</b> | <b>BENEFIT OF THE STUDY FOR THE NILE BASIN INITIATIVE</b> .....                        | <b>71</b> |
| <b>7</b> | <b>CONCLUSIONS AND RECOMMENDATIONS</b> .....   | <b>73</b> |
| 7.1      | CONCLUSIONS .....  | 73        |
| 7.2      | RECOMMENDATIONS .....  | 75        |
|          | <b>REFERENCES</b> .....  | <b>77</b> |
|          | <b>ANNEXES</b> .....   | <b>81</b> |
|          | ANNEX A: MONTHLY RAINFALL DATA OF KUNZILA STATION .....                                | 82        |
|          | ANNEX B: TANA-BELES PROJECT SITE MAP (ADOPTED FROM TANA BELES PROJECT .....            | 83        |
|          | ANNEX-C: MONTHLY RAINFALL SERIES IN AND AROUND BELES SUB BASIN (1980/81 -1999/2000) .. | 84        |
|          | ANNEX-D: DAILY FLOW RECORD TIME SERIES OF MAIN BELES RIVER AT BRIDGE .....             | 85        |

## List of symbols /Acronyms

|          |  |
|----------|--|
| AOGCM-   | Atmosphere-Ocean General Circulation Model                   |
| ClimGEN- | Climate Generator model                                      |
| GCM-     | General Circulation Model                                    |
| HadCM3   | Hadely Center Coupled Model, version 3                       |
| HEC      | HMS-Hydrologic Engineering Center-Hydrologic Modeling System |
| IPCC     | Intergovernmental Panel on Climate Change                    |
| ITCZ     | Inter Tropical Convergence Zone                              |
| MASL     | Mean Annual sea Level  |
| MOWR     | Ministry of Water Resource, Ethiopia                         |
| NCEP     | National Center for Environmental Prediction                 |
| RCM-     | Regional Circulation Model                                   |
| SDSM     | Statistical Downscaling Model                                |
| SRES-    | Special Report on Emission Scenarios                         |
| TLFN-    | Time Lagged Feed forward neural network                      |
| LARS-    | WG-Long Ashton Research Station Weather Generator            |



## Lists of Figures

|   |    |
|---|----|
| <i>Figure 2. 1 Beles Basin location in Ethiopian map</i> .....  | 5  |
| <i>Figure 2. 2 Tana and Beles Basin Map (source:(SMEC, 2008))</i> .....   | 6  |
| <i>Figure 2. 3 Upper Main Beles and Gilgel Beles sub-basins</i> .....   | 6  |
| <i>Figure 2. 4: Land use Map</i> .....  | 8  |
| <i>Figure 2. 5: land cover in the Upper Beles Sub-Basin</i> .....   | 8  |
| <i>Figure 2. 6: Soil Map</i> .....  | 9  |
| <i>Figure 2. 7: Gilgel Beles 1243 dam and Gilgel Beles 1243 water treatment plant</i> .....   | 11 |
| <i>Figure 2. 8: Beles 1025 weir</i> .....   | 11 |
| <i>Figure 2. 9 Potential Irrigation sites in the Beles basin</i> .....  | 12 |
| <i>Figure 2. 10 Tana-Beles Hydropower project under construction</i> .....  | 13 |
| <i>Figure 2. 11 Location Map of Beles Hydropower (BHP), Beles 1243 dam (B 1243) and Beles 1025 weir (B 1025)</i> .....  | 13 |
|   |    |
| <i>Figure 4. 1: Meteorological stations in and around Upper Beles Basin</i> .....   | 25 |
| <i>Figure 4. 2 Hydrological gauging stations in the Tana and Beles Basins (source SMEC)</i> .....   | 26 |
| <i>Figure 4. 3 Semi-empirical distribution used by LARS-WG (histogram)</i> .....  | 30 |
| <i>Figure 4. 4: African continent Windows with 2.5<sup>o</sup> latitude x 3.75<sup>o</sup> Longitude from which grid of study area selected shown in black square box</i> ..... | 33 |
| <i>Figure 4. 5:Time-lagged feed-forward network (TLFN) adopted from (Muluye and Coulibaly, 2007)</i> .....  | 37 |
| <i>Figure 4. 6: Conceptual schematic of the continuous soil moisture accounting algorithm (Bennett, 1998) (source HEC-HMS Technical manual)</i> .....                           | 39 |
| <i>Figure 4. 7: The three small sub-basins of Upper Main Beles</i> .....  | 42 |
| <i>Figure 4. 8 : Thiession polygon for Upper main Beles sub-basin</i> .....   | 43 |
|   |    |
| <i>Figure 5. 1 Observed and generated rainfall for Mandura station using ClimGen model</i> .....  | 47 |
| <i>Figure 5. 2: T-test of annual rainfall of Bhardar station</i> .....  | 49 |
| <i>Figure 5. 3 Changing point test of annual rainfall of Bhardar station</i> .....  | 49 |
| <i>Figure 5. 4: Validation result of SDSM model downscaling of daily precipitation and maximum temperature at Pawe station at Pawe station</i> .....                            | 52 |
| <i>Figure 5. 5 : Pawe rainfall increase/ decrease in percentage for A2scenrio</i> .....   | 54 |
| <i>Figure 5. 6: Pawe rainfall increase/ decrease in percentage for B2scenrio</i> .....  | 54 |
| <i>Figure 5. 7: General trend in maximum temperature corresponding to A2a scenario</i> .....  | 55 |
| <i>Figure 5. 8: General trend in maximum temperature corresponding to B2a scenario</i> .....  | 55 |
| <i>Figure 5. 9 : General trend in minimum temperature corresponding to A2a scenario</i> .....   | 56 |
| <i>Figure 5. 10: General trend in minimum temperature corresponding to B2a scenario</i> .....   | 56 |
| <i>Figure 5. 11: Sensitivity of a TLFN (in downscaling precipitation at Pawe stations) to each of the predictors variables used as input to the network</i> .....               | 57 |
| <i>Figure 5. 12 Validation results of TLFN downscaling daily rainfall, maximum and minimum temperature at Pawe station</i> .....  | 59 |
| <i>Figure 5. 13: General trend in max temperature corresponding to A2a scenario</i> .....   | 60 |
| <i>Figure 5. 14: General trend in min temperature corresponding to A2a scenario</i> .....   | 60 |
| <i>Figure 5. 15 Simulated and observed flow hydrographs</i> .....   | 62 |
| <i>Figure 5. 16 Observed vs. simulated (calibration)</i> .....  | 63 |
| <i>Figure 5. 17: Simulated and observed flow in model calibration (stochastic calibration)</i> .....  | 63 |
| <i>Figure 5. 18 : Simulated and observed flow hydrographs</i> .....   | 64 |
| <i>Figure 5. 19 observed vs. simulated (validation)</i> .....   | 64 |
| <i>Figure 5. 20: Comparison of average mean monthly and percentage flow change –A2a scenario</i> .....  | 66 |
| <i>Figure 5. 21: Percentage change in stream flow for B2a scenario</i> .....  | 67 |



## List of Tables

|  |    |
|--|----|
| <i>Table 3. 1 Comparative summary of the relative merits of statistical and dynamical downscaling techniques adapted from (Fowler et al., 2007; Wilby and Wigley, 1999)</i> .....  | 18 |
| <i>Table 3. 2: Percentage change (from baseline) in flow and rainfall during wet season (June–September)</i> .....   | 22 |
| <i>Table 3. 3 Changes in climatic variables and runoff for the 2050s</i> .....   | 23 |
| <br>   |    |
| <i>Table 4. 1: List of Predictor variables derived from African window for the grid on the study area (Twenty six predictor variables)</i> .....   | 34 |
| <br>   |    |
| <i>Table 5. 1: Correlation matrix of the three meteorological stations using daily,</i> .....  | 45 |
| <i>Table 5. 2: Output data from the statistical tests, showing the comparison of the observed rainfall, &amp; maximum temperature monthly means and variances with those of 20 years of synthetic data generated by LARS-WG for Mandura station.</i> ..... | 46 |
| <i>Table 5. 3 : ClimGen Results of the statistical tests showing the comparison of the observed precipitation and maximum temperature means and variances with those of 20 year synthetically generated data by ClimGen at Mandura station</i> .....       | 47 |
| <i>Table 5. 4: Results of F-test and T-test for annual rainfall, max and min temperature of Bhardar stations. X indicates absence of significant change points</i> .....   | 48 |
| <i>Table 5. 5 List of predictor variables that have better spatial and temporal correlation with the predictands at Pawe station with significant level less than 0.05(<math>p &lt; 0.05</math>)</i> .....   | 51 |
| <i>Table 5. 6 :List of predictor variables that have better spatial and temporal correlation with rainfall as predictand for Bhardar and Dangila station with significant level less than 0.05(<math>p &lt; 0.05</math>)</i> .....                         | 51 |
| <i>Table 5. 7: Model validation statistics with observed data and Large scale Re-analysis data</i> .....   | 52 |
| <i>Table 5. 8: sensitive predictor variables</i> .....   | 58 |
| <i>Table 5. 9 Model validation statistics</i> .....  | 58 |
| <i>Table 5. 10 Optimal model calibration parameters</i> .....  | 62 |
| <i>Table 5. 11 Summary of Irrigation water requirements for the two irrigation seasons</i> .....   | 68 |
| <i>Table 5. 12: stream flow change under synthetic scenario</i> .....  | 69 |





# 1 Introduction

## 1.1 Background

Climate change is one of the greatest environmental, social and economic threats facing our planet today. Human activities, in particular the burning of fossil fuels (coal, oil and gas), are believed to increase the atmospheric concentrations of greenhouse gases. In its Fourth Assessment Report (AR4), published in February 2007, the Intergovernmental Panel on Climate Change (IPCC, 2007) indicates that, without further action to reduce greenhouse gas emissions, the global average surface temperature is likely to rise by a further 1.8-4.0°C in 21<sup>st</sup> century.

As a consequence of Global warming climate change will intensify the hydrological cycle in ways that have substantial impacts on water resource availability and water quality (Miller and Yates, 2004). Changes in water resource availability will in turn affect water management, allocations, and reliability. Water resource planning based on the concept of a stationary climate is increasingly considered inadequate for sustainable water resources management unless regional climate studies are included at river basin level (Mohammed *et al.*, 2005). Therefore quantitative estimates of hydrologic effects of climate change on river basin level are essential for understanding and solving potential water resource management problems associated with water supply for domestic and industrial water use, power generation, and agriculture as well as for future water resource planning, reservoir design and management, and protection of the natural environment

A number of studies have been conducted on the Nile River; however, very few studies have investigated the impact of climate change on Upper Blue Nile River Basin (Ethiopia). There appears to be no literature published at sub-basin levels. All studies were focused on the whole basin. But the water resource planning and managements are carried out at the sub- basin levels. The use of watershed as the basic planning and data aggregation and computational unit not only allows the integration of water uses and water supplies, but it is also important in managing the relationship between quantity and quality and upstream and downstream water interests. This study is carried out in the Beles sub- basin. Beles sub -basin is one of the major tributary of upper Blue Nile river basin, which is the main water source of Nile River flow. It is one of the potential future development areas with untapped water resource potential. Currently Tana Beles Multi purpose hydropower project through inter basin water transfer from Lake Tana is under construction and Upper Beles irrigation project is also on the way. Therefore assessing the climate change impact in the basin is essential for adaptive water resource planning and management

## **1.2 Problem statement**

One of the most important consequences of climate change will be alterations in major climate variables, such as temperature, precipitation, and evapotranspiration. This in turn will lead to changes in the hydrological cycle, influencing the components of water balance of drainage basins in several ways such as the availability and distribution of water resources in space and time, stream flow, frequency of extreme events etc.

Research has shown that Blue Nile flow is sensitive to climate change. Beles River, the major tributary of upper Blue Nile is one of the future development areas. Therefore assessing the possible impact of climate change on the stream flow of this river is essential for future development as well as for managing the current water resource development projects in adaptive way. This study uses statistical downscaling technique and hydrological model to simulate the possible impact of climate change on the stream flow of Beles River.

## **1.3 Research Objectives**

The main objective of this research is to downscale the Global Circulation Model (GCM) output in particular temperature and precipitation to regional or watershed level for analyzing the impact of climate change on stream flow of Beles River using HEC-HMS rainfall-runoff model.

Specific objectives:

- Downscaling GCM model output to regional level
- Developing temporal climate change scenario for the future
- Building rainfall-runoff model for the watershed
- Assessing the possible climate change impact on the stream flow
- Assessing the potential climate change impact on the water resource development such as on Irrigation projects.

## **1.4 Structure of the Thesis**

Impact of climate change on the hydrological cycle and its implication to water resource management, problem statement and objectives of the study are given in the first chapter. Description of the study area are provided in Chapter 2

The third chapter gives a review on Global climate models (GCM), Downscaling methods, climate scenarios and previous climate change studies in Blue Nile.

In the fourth chapter data screening, weather generation models for filling missing data, GCM model used, description of statistical downscaling model, Time lagged feed forward neural networks for downscaling and HEC-HMS hydrological model are presented

Chapter 5 presents the results and discussion part of the thesis in five sections

Data analysis, comparative results of weather generator models are presented in the first section. In the second section comparative result of statistical downscaling model and Time lagged Feed forward neural network are given. HEC-HMS hydrologic model results including stream flow impact assessment based on future climate scenarios, are presented in the third section. In the last sections crop water requirements based on future development scenarios and sensitivity analysis based on incremental scenario are presented.

Chapter 6 presents the importance of the study to the Nile Basin Initiative.

Conclusions and recommendations are given in chapter 7. In this chapter conclusions based on results are given and further studies on the limitations encountered have been suggested for future research.



## 2 Description of the study area

Beles basin is one of the major sub-basins of upper Blue Nile. The main stem of the Beles River originates on the face of the escarpment across the divide to the west of the south-western portion of Lake Tana. It then flows on in a westerly direction and enters into the Blue Nile just before it crosses the Ethiopia-Sudan frontier. It is the only major right bank tributary of Blue Nile. The Beles basin covers an area of about 14,000 km<sup>2</sup> and geographically it extends from 10° 56' to 12° N latitude and 35°12' to 37° E longitude. The basin has two gauged sub-catchments, Main Beles and Gilgile Beles that have a size of 3474 km<sup>2</sup> and 675 km<sup>2</sup> respectively. In particular the main focus of this study is the gauged part of the basin called Upper Beles sub-basin. Figure 2.1 shows the location of Beles basin in Ethiopian map, Figure 2.2 shows the Tana and Beles basin and Figure 2.3 shows the Upper Beles sub-basins (Upper main Beles and Gilgile Beles sub-basins)



Figure 2. 1 Beles Basin location in Ethiopian map

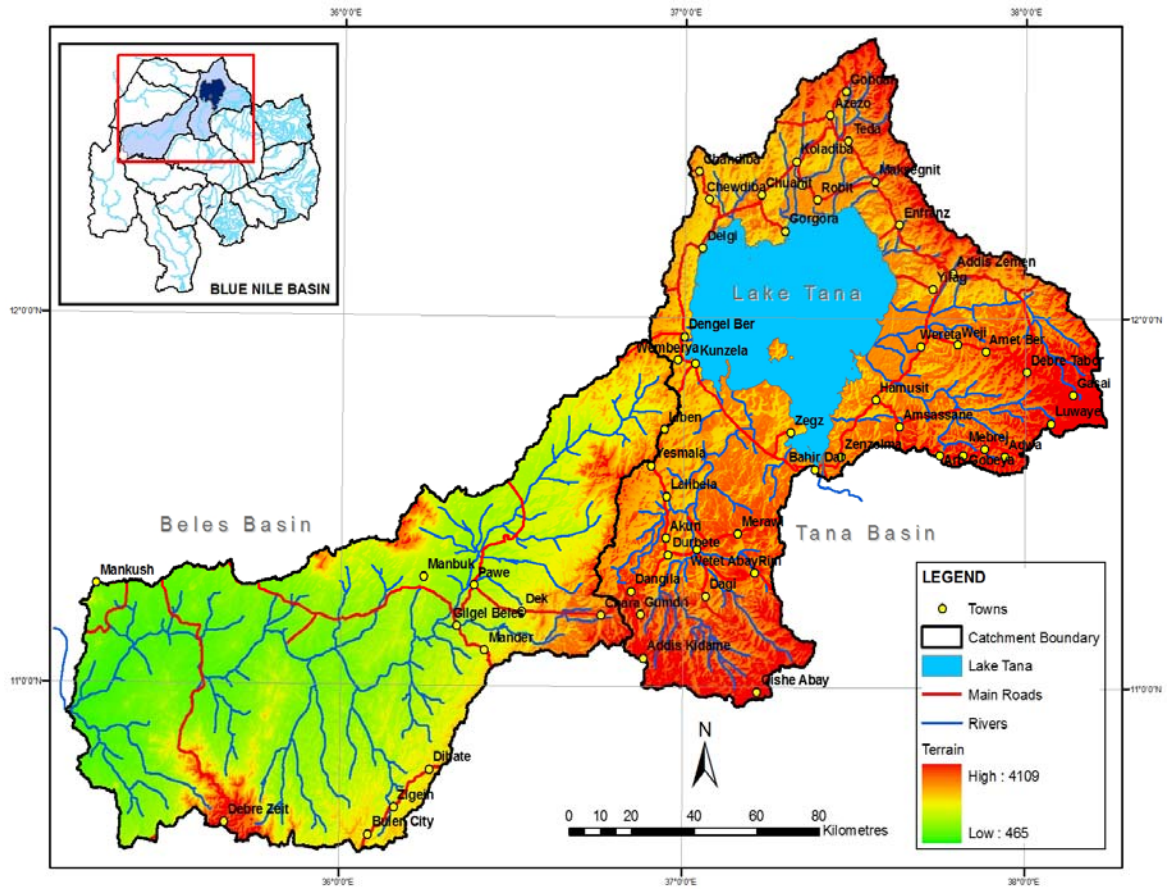


Figure 2. 2 Tana and Beles Basin Map (source:(SMEC, 2008))

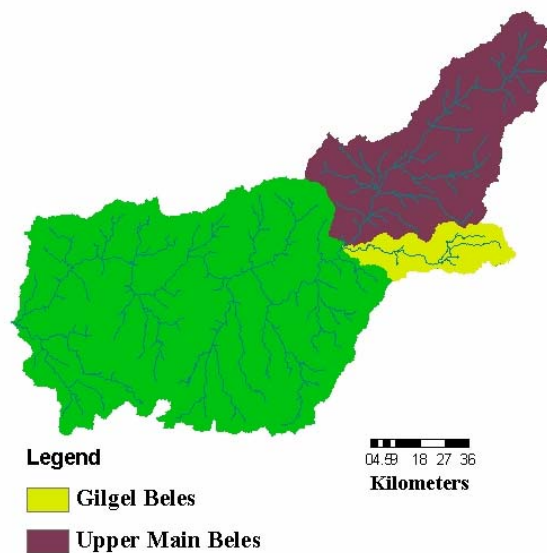


Figure 2. 3 Upper Main Beles and Gilgel Beles sub-basins

## **2.1 Topography**

The Upper Beles sub basin is bounded on the east and south east by steep escarpment and on the north and west by rolling to hilly terrain which separates it from the Dindir River drainage basin. The highest point in the Basin is 2,725 AMSL at the water divide between the Tana and Beles basins and the mean elevation is about 1870 AMSL .The central part of this watershed encloses the wide, gently undulating to flat plains of the Pawe area.

## **2.2 Climate**

The climate of Ethiopia is very much the reflection of its diversified topography and its location in the tropics. Climate seasons of the country are mainly controlled by the annual migration of the InterTropical Convergence Zone (ITCZ) and the associated atmospheric circulation, which are modulated by the complex topography on the region (Geathun, 2007).

Three main seasons characterize Ethiopia (NMSA, 2001). These are (1) ITCZ that drives the summer monsoon in the wet season from June to September, locally called Kiremt; (2) Saharan anticyclone that generates dry, warm and cool northeasterly winds in the dry season from October to January or February, called Bega and (3) Arabian high that produces thermal lows in the mid season from February or march to may called Belg.

The climate in the study area is warm and subtropical. The annual mean yearly minimum and maximum temperature is ranging between 16.5°C- 32.5 °C (Pawe metro. station). Precipitation is moderately abundant (about 1000 mm/year), even in years when other adjacent areas are very severely affected by drought. Rainfall increases with elevation in the study area. Annual potential evapotranspiration is about 1500 mm.

## **2.3 Land use**

The land use of the study area can be categorized mainly as agricultural, forest, bamboo, bushes, and savanna. The upper Blue Nile Master plan study(USBR, 1964) indicates that the north-western portion of the area is dominated by open grass savannah where as the southern half of the basin is characterized by wood-land savannah composed of various species of acacia, figs, and associated small trees. As it can be seen in (Figures 2.4) the Upper Main Beles sub-basin is dominated by open grassland. Figure 2.5 also shows the land cover in the sub-basin as observed during field visit.

According to the information collected during the field visit from the Agricultural research centre of Pawe, farming system in the study area can be described as mixed crop livestock production. The principal crops grown in the area by the local population includes finger millet, teff, sorghum and maize while minor crops include nugga, chick pea, and sesame

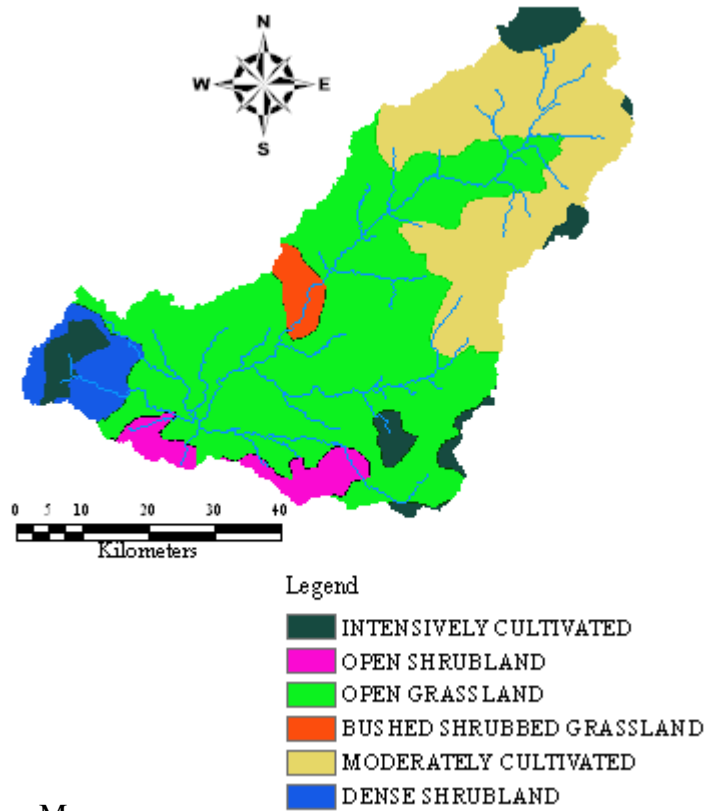


Figure 2. 4: Land use Map



Figure 2. 5: land cover in the Upper Beles Sub-Basin



## 2.4 Soil

Black clay soils are predominant in the Beles River Basin and particularly in the north-western area where topographic conditions are best suited for irrigation. Upper Beles sub-basin near Pawe plateau is more dominated by Chromic Vertisols and Chromic Luvisols are more dominant at the upper part of the sub-basin (Figure 2.6).

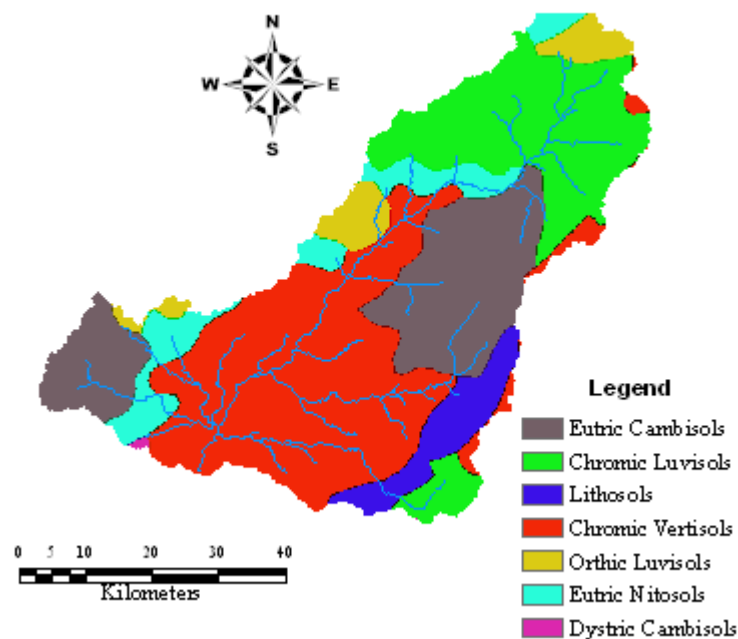


Figure 2. 6: Soil Map

## 2.5 Drainage Networks

The Upper Beles Sub basin is comprised of two main rivers namely Main and Gilgel Beles. The head water of Beles River starts from the area close to the western periphery of Lake Tana. Along its way it collects many major and minor tributaries. Gezhig, Burzhi and Chankur, Bula (keteb) and Giligile Beles are the major tributaries. The drainage networks can be viewed in Annex: B,

## 2.6 Tana Beles project

Tana Beles project as a multipurpose project was initially conceived in the study and survey report made by the United States Bureau of Reclamation on the land and water resources of the Blue Nile Basin in 1958 and 1964 respectively. The project has never been realized until the time when the country was affected by the disastrous drought and famine in 1984/85 which was followed by a massive resettlement program

launched by the Ex-Government of Ethiopia. The scale of the tragedy caused by the drought and famine in the country has attracted the attention of the international communities. On positive response was made by the Italian Government to support those regions in the Sahel in their effort to with stand the drought and its consequences(Tefferra *et al.*, 1992).

An area of 19,000 ha of land was identified between Lake Tana and Blue Nile, 500 km north-west of Addis Ababa, covered with rich vegetation and with particularly favorable climatic and soil conditions. In this unexplored area, through which the river Beles runs, it was decided to launch an agro-industrial program the aiming at developing a flourishing food reservoir, capable of supplying food to local people, and eventually to the rest of the country. A year after the commencement of the Beles valley emergency resettlement, on the 29<sup>th</sup> of March 1986 the Italian Government-funded project known as the “Tana Beles Project” officially began its work (SaliniCostruttori, 1989).

Deboch (2002) has noted that except for its later serious drawbacks on the sustainability of its top-down and high-tech interventions; initially the operation of the project has greatly improved the emergency conditions of the resettlement area. Since the project was developed in the Derg regime’s development policy framework, it has emphasized agricultural collectivisation. Additionally the project was criticized for high tech centralized approach

Hence critically commenting on these short comings of the project Agneta et al(1993 ) cited in (Deboch, 2002) noted the following

“The Beles project focused mainly on the infrastructure development of the area where people had already been moved, rather than proposing a range of solutions to basic problems such as the self-sustainability of the households, the diversifications of the farming systems, the integration of the resettlement area in to regional economy, and negotiation of conflicts deriving from host-settlers disputes over land use and over the share of benefit resulting from the project”.

It is beyond the scope of this study to address the issues of sustainability of the Tana Beles project .For informative purposes, however, the water resource development schemes constructed during the Tana Beles project are presented in the following sections.

### **Gilgel Beles 1243**

Giligile Beles 1243 dam is a dam constructed on Giligile Beles River for providing drinking water supply (Figure 2.7). It is located at elevation of 1243m AMSL which is at higher elevation with respect to the project area to enable gravity water supply. Gilgel Beles 1243 dam is a concrete gravity dam with two overflow spillways, bottom

outlet and flap gate which are operated by hydraulic system. It diverts water to Gilgel Beles 1243 water treatment plant which is a slow sand filter type treatment plant constructed just downstream of this dam for treating the diverted water. Currently both the dam and the treatment plant are hardly operational.



Figure 2. 7: Gilgel Beles 1243 dam and Gilgel Beles 1243 water treatment plant

### **Beles 1025 weir**

Beles 1025 weir (Figure 2.8) is located at a distance of about 3km from Pawe town. It is an ogee weir constructed for irrigation purpose and to supply water to other irrigation schemes. The weir is not completed and has not yet started working. But the structures are in good condition and the system can be upgraded with relative ease. Its location can be seen in Figure 2.11



Figure 2. 8: Beles 1025 weir

## Current status of Tana Beles project

The current main water resource development projects in the Upper Beles basin include Tana-Beles Hydropower and Upper Beles Irrigation projects. The Tana-Beles Hydropower project is designed to exploit the huge natural storage capacity of Lake Tana and the elevation difference between the Lake Tana and the Upper Beles valley of some 330m through inter-basin transfer to generate 1540 GWh of firm electrical energy per year. The power scheme is essentially a single stage development and, apart from an intake approach channel and appurtenant structures on the shores of Lake Tana it includes construction of five low re-regulating weirs in the Jehana valley, (a tributary of the Beles River). Figure 2.10 shows the current status of the project under construction). Figure 2.11 shows the location map of Beles1025 weir, Beles 1243 dam and Beles Hydropower

The other main water resource development project in the area under study is the Upper Beles Irrigation project. It is located on the upper part of Beles river basin and extends on both sides of river Beles. Since the irrigation project area is being on the upper part of the drainage basin, the Beles river would provide only an insignificant amount of water compared to the requirements for the irrigable land. Therefore it is planned to utilize a portion of the water discharged from the power plant for irrigation only and the balance to by pass farther downstream. The potential land for irrigation is estimated as 123,000 ha. Figure 2.9 shows the potential irrigation land in Beles basin

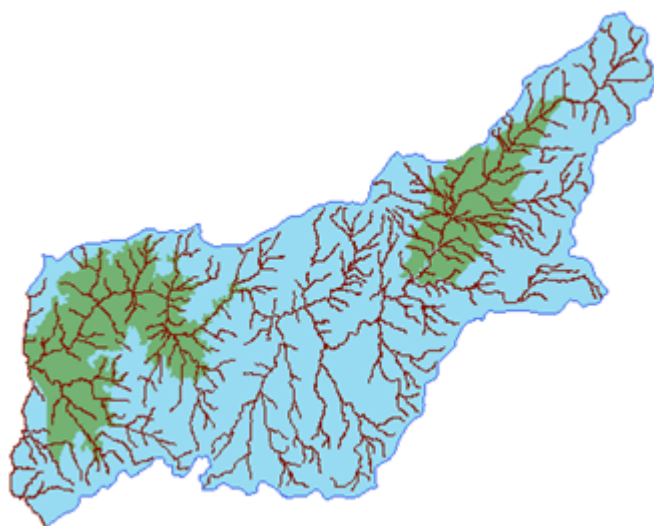


Figure 2. 9 Potential Irrigation sites in the Beles basin



(a) Approach channel at Lake Tana

(b) Underground powerhouse

Figure 2. 10 Tana-Beles Hydropower project under construction



Figure 2. 11 Location Map of Beles Hydropower (BHP), Beles 1243 dam (B 1243) and Beles 1025 weir (B 1025)

All this water resource development projects may be influenced by climate change. Their long term performance may be altered if the existing climatic conditions are changed. Therefore this study is relevant for current as well as future developments in the sub-basin



## **3 Literature Review**

### **3.1 Global Climate Change**

Climate change refers to a change in the state of the climate that can be identified (e.g., using statistical tests) by changes in the mean and/or the variability of its properties, and that persists for an extended period, typically decades or longer. It may be due to internal processes or external such as change in solar radiation and composition of the atmosphere(IPCC, 2007).

Emissions of greenhouse gases and aerosols due to human activities continue to alter the atmosphere in ways that are expected to affect the climate. Human activities contribute to climate change by causing changes in Earth's atmosphere in the amounts of greenhouse gases, aerosols (small particles), and cloudiness. The largest known contribution comes from the burning of fossil fuels, which releases carbon dioxide gas to the atmosphere(IPCC, 2007). In the same report it is also indicated that the Global mean surface temperature has increased by about 0.74°C [0.56°C to 0.92°C] over the past hundred years (between 1906 and 2005) and without further action to reduce greenhouse gas emission the global average surface temperature is projected to be likely increased further by 1.8- 4.0°C this century.

### **3.2 Climate Models**

Climate models apply simplified representations of the physical laws governing mass and energy exchanges in the ocean-atmosphere system enabling us to better understand and predict the consequence of greenhouse gas emissions. The mathematical models generally used to estimate the present climate and project future climate with forcing by greenhouse gases and aerosols are generally referred to as Global Circulation Model (GCM). In general, most GCMs simulate global and continental scale processes and provide a reasonably accurate representation of the average planetary climate. Nevertheless, while GCMs demonstrated significant skills at the continental and hemispherical scales and they incorporate a large portion of the complexity of the global system, they are inherently unable to represent local sub-grid scale features and dynamics Wigley et al 1990, Carter et al 1994; cited in (Dibike and Coulibaly, 2005).

The mismatch in scales between GCM resolution and the increasingly small scales required by impact analysts can be overcome by downscaling (Wilby and Wigley, 1999)

Model simulations in to the future “predictions” depend on assumptions regarding future anthropogenic emissions of greenhouse gases, which in turn depend on assumptions about many factors involving human behaviour. Therefore it has been thought inappropriate and possibly misleading to call the simulations of future climate so far ahead ‘predictions’. They are instead called ‘projection’ to emphasize that what is being done is to explore likely future climates which arise from a range of assumptions regarding human activities (Houghton, 2004)

### **3.3 Downscaling**

As discussed in the previous section Global Climate Models (GCMs) have a resolution of hundreds of kilometers; however, climate change information is required for many impact studies at a spatial scale of much finer than those provided by GCMs (Dibike and Coulibaly, 2005). Therefore downscaling techniques have emerged as a means of relating meso-scale atmospheric variables to grid and sub-grid scale surface variables .There are two main approaches for deriving information on local or regional scales from the global climate scenarios generated by GCMs (Wilby and Wigley, 1999). Numerical downscaling (also know as dynamic downscaling) involving a nested regional climate model (RCM) and statistical downscaling employing statistical relationship between the large-scale climatic state and local variations derived from historical data records. These two approaches are discussed in the following sections.

#### **3.3.1 Dynamic downscaling**

Dynamical downscaling involves the nesting of a finer-scale regional climate model, also called limited area models (LAMs) within the coarser global climate model. A dynamic approach uses the output of GCM as boundary conditions for the region of interest. A fully physical climate model is then used to calculate future climate at regional scale. An important advantage of dynamical models is that they account for local conditions, which may include changes in land-surface vegetation or atmospheric chemistry in physically consistent ways. However Regional climate models (RCMs) are computationally demanding, requiring as much processor time as the GCM to compute equivalent scenarios and are not easily transferred to new regions. The results from RCMs are also sensitive to choice of the initial conditions (especially soil moisture and soil temperature) used at the start of the experiment (O'Hare *et al.*, 2005)

Fowler et al (2007) also noted that RCMs are able to realistically simulate regional climate features such as orographic precipitation, extreme climate events and regional scale climate anomalies. Model skill depends strongly on biases inherited from the driving GCM and the presence and strength of regional scale forcings such as orography, land-sea contrast and vegetation cover.



Mohammed (2005) has applied regional climate model called (RACMO) over the Nile Basin and reported that the model is reasonably well in producing the runoff of the Blue Nile and Atbara sub-basin where as it shows overestimation in White Nile runoff.

### **3.3.2 Statistical downscaling**

Statistical downscaling involves developing quantitative relationships between large-scale atmospheric variables (predictors) and local surface variables (predictand) (Wilby *et al.*, 2004). The most common form has predictand as a function of the predictors. Statistical downscaling seeks to derive the local information from the larger scale through inference from the cross-scale relationship using some random or deterministic functions. In most cases, the regional climate is seen as random process conditioned upon a driving large-scale climate regime. Therefore, the confidence that may be placed in downscaled climate change information is foremost dependent on the validity of the large-scale fields from GCM. For instance, derived variables such as precipitation are usually not robust information at the regional and local scale where as tropospheric quantities such as temperature or geopotential height are intrinsic parameters of GCM physics and are more skilfully represented by GCMs (Coulibaly and Dibiye, 2004)

According to Wilby and Wigley(1999) the following assumptions are involved in statistical downscaling: (i) suitable relationships can be derived between large scale and small scale predictor variables (ii) these observed empirical relationships are valid under future climate conditions and (iii) the predictor variables and their change are well characterized by GCMs.

A diverse range of statistical downscaling techniques have been developed over the past few years and each method generally lies in one of the three categories, namely regression(transfer function) methods , stochastic weather generators and weather typing schemes (Wilby *et al.*, 2004)

Table 3.1 presents the comparative advantage and disadvantage of statistical and dynamical downscaling methods

Table 3. 1 Comparative summary of the relative merits of statistical and dynamical downscaling techniques adapted from (Fowler *et al.*, 2007; Wilby and Wigley, 1999)

| Statistical downscaling  | Dynamical downscaling  |
|--|--|
| <p>Advantages</p> <ul style="list-style-type: none"> <li>• Comparatively cheap and computationally efficient</li> <li>• Can provide point-scale climatic variables from GCM-scale output</li> <li>• Can be used to derive variables not available from RCMs</li> <li>• Easily transferable to other regions</li> <li>• Based on standard and accepted statistical procedures</li> <li>• Able to directly incorporate observations into method</li> </ul>                                 | <ul style="list-style-type: none"> <li>• Produces responses based on physically consistent processes</li> <li>• Produces finer resolution information from GCM-scale output that can resolve atmospheric processes on a smaller scale</li> </ul> |
| <p>Disadvantages</p> <ul style="list-style-type: none"> <li>• Require long and reliable observed historical data series for calibration</li> <li>• Dependent upon choice of predictors</li> <li>• Non-stationarity in the predictor-predictand relationship</li> <li>• Climate system feedbacks not included</li> <li>• Dependent on GCM boundary forcing; affected by biases in underlying GCMs</li> <li>• Domain size, climatic region and season affects downscaling skill</li> </ul> | <ul style="list-style-type: none"> <li>• Computationally intensive</li> <li>• Limited number of scenario ensembles available</li> <li>• Strongly dependent on GCM boundary forcing</li> </ul>  |

### 3.4 Climate scenarios

Climate scenarios are plausible representations of the future that are consistent with assumptions about future emissions of greenhouse gases and other pollutants, and with our understanding of the effect of increased atmospheric concentrations of these gases on global climate (IPCC-TGCI, 1999). A range of scenarios can be used to identify the sensitivity of an exposure unit to climate change and to help policy makers decide on appropriate policy response. Climate scenarios are not predictions. Rather climate scenarios were created because there is much less confidence in estimates of how climate will change at regional scale and there is no confidence in predicting climate changes at these scales.

IPCC-TGCI (1999) mentions three types of scenarios that have been applied in impact assessments: synthetic scenario, analogue scenario, and scenarios based on output from GCMs.

Synthetic scenarios (Incremental scenarios) are scenarios that describe techniques where particular climatic (or related) elements are changed by realistic but arbitrary amount (e.g. +1, 2, 3, 4 °C from the baseline temperature and ±5, 10, 15 and 20% change from the baseline precipitation). Analogue scenarios are scenarios constructed by identifying recorded climate regimes which may resemble the future climate in a given region. There are two types of analogue scenarios; temporal analogue, based on information from geologic records such as fossil evidence and spatial analogue are based on regions which today have a climate analogue to the study region in the future. The last scenario, using the GCM model output is the most common method of developing climate scenarios for quantitative impact assessments, which is also the objective of this study.

### **3.4.1 Emissions Scenarios**

It is difficult to know exactly how anthropogenic emissions will change in the future. However, the IPCC Special Report on Emission Scenarios (SRES) has developed new emission scenarios, the so called “SRES scenarios”. Emission scenarios are plausible representations of future emissions of greenhouse gases or sulphur dioxide which forms sulphate aerosols (Richard Jones *et al.*, 2004). These are based on a coherent and internally consistent set of assumptions about driving forces (such as demographic and socio-economic development and technological change) and their key relationships. The SRES scenario set comprises four scenario families: A1, A2, B1 and B2. The scenarios within each family follow the same picture of world development (“storyline” – see Box 1). The A1 family includes three groups reflecting a consistent variation of the storyline (A1T, A1FI and A1B). Hence, the SRES emissions scenarios consist of six distinct scenario groups, all of which are plausible and together capture the range of uncertainties associated with driving forces<sup>1</sup>

---

<sup>1</sup> <http://www.grida.no/climate/ipcc/emission/030.htm>(IPCC)

## **Box 1: The Main Characteristics of the Four SRES Storylines and Scenario Families<sup>2</sup>**

The SRES Scenarios are based on a set of four different storylines within each of which a family of scenarios has been developed-leading to a total of forty scenarios  
All scenario groups are equally sound

### **A1 Storyline**

The A1 storyline and scenario family describes a future world of very rapid economic growth, low population growth, and the rapid introduction of new and more efficient technologies. Major underlying themes are convergence among regions, capacity building, and increased cultural and social interactions, with a substantial reduction in regional differences in per capita income. The A1 scenario family develops into four groups that describe alternative directions of technological change in the energy system.

### **A2 Storyline**

The A2 storyline and scenario family describes a very heterogeneous world. The underlying theme is self-reliance and preservation of local identities. Fertility patterns across regions converge very slowly, which results in high population growth. Economic development is primarily regionally oriented and per capita economic growth and technological changes are more fragmented and slower than in other storylines.

### **B1 Storyline**

The B1 storyline and scenario family describes a convergent world with the same low population growth as in the A1 storyline, but with rapid changes in economic structures toward a service and information economy, with reductions in material intensity, and the introduction of clean and resource-efficient technologies. The emphasis is on global solutions to economic, social, and environmental sustainability, including improved equity, but without additional climate initiatives.

### **B2 Storyline**

The B2 storyline and scenario family describes a world in which the emphasis is on local solutions to economic, social, and environmental sustainability. It is a world with moderate population growth, intermediate levels of economic development, and less rapid and more diverse technological change than in the B1 and A1 storylines. While the scenario is also oriented toward environmental protection and social equity, it focuses on local and regional levels.

---

<sup>2</sup> <http://www.grida.no/climate/ipcc/emission/030.htm>(IPCC)

### 3.5 Key Uncertainties in Climate Scenarios

Richard Jones et al (2004) have discussed five types' of uncertainties in climate change scenarios for assessing the impacts of climate change.

**Uncertainties in future emissions scenarios:** These are due to the key assumptions about and relationships between future population, socio-economic development and technological change that are the bases of the IPCC SRES Scenarios. They can be allowed for by making climate projection for a range of these SRES emissions scenarios.

**Uncertainty in future concentrations:** These are due to imperfect understanding of some of the processes and physics in the carbon cycle and chemical reactions in the atmosphere that generates uncertainties in the conversion of emissions to concentration. To reflect this uncertainty in the climate scenarios, the use of atmosphere-ocean general circulation models (AOGCMs) that explicitly simulate the carbon cycle and chemistry of all the substances are needed.

**Uncertainty in response of climate:** There is much we do not understand about the workings of the climate system, and hence uncertainties arise because of our incorrect or incomplete description of key processes and feedbacks in the model. This is clearly illustrated by the fact that current global climate models, which contain different representations of the climate system, project different patterns and magnitudes of climate change for the same period in the future when using the same concentration scenarios. For this reason it is strongly recommend using a number of different GCMs as input to climate impacts studies.

**Uncertainty due to natural variability:** The climate varies on timescales of years and decades due to natural interactions between atmosphere, ocean and land, and this natural variability is expected to continue into the future. This uncertainty cannot yet be removed, but it can be quantified. This is done by running ensembles of future climate projections; by initiating each run from a different starting point in the "control" climate. The results of this ensemble for a particular 10- or 30-year period will give a range of possible futures which are likely to span the actual evolution of the climate system, assuming the representation in the climate model to be correct.

**Uncertainty in regional climate change:** all regionalization techniques carry with them the errors from the driving GCM fields although this is not an uncertainty in regionalization, it must be borne in mind. Different regionalization techniques can give different local projections, even when based on the same GCM projection. Even with the same technique, different RCMs will give different regional projections, even when based on the same GCM output.

### 3.6 Climate change studies on Blue Nile

To date, several investigators have carried out climate change impacts assessments for the Nile basin. This section reviews some of the findings on the impact of climate change on Upper Blue Nile.

Nawaz and Bellerby (2007) have carried out a study on the sensitivity of Blue Nile flow to climate change using the output of three GCM models; CGCM2, ECHAM4, HADCM3 and SERS emission scenarios (A2 and B2). They used histogram matching (Multidimensional Stochastic Rainfall Generator) for downscaling and Nile forecasting distributed hydrological model for impact assessment.

They found general increase in rainfall for 2020s in all the models but by 2050s they have observed different patterns between the models, the CGCM indicates drier conditions whilst the ECHAM and HadCM3 indicate wetter conditions. ECHAM in particular indicates very wet conditions especially under the B2 scenario. And by 2080s the ECHAM B2 scenario in particular, indicates a very wet future whilst CGCM2 results in very dry conditions. The HadCM3, on the other hand, still provides relatively modest changes (increases).

They found percentage change in mean flow variation from -46.6% (CGCM A2 2080s) to +12.4% (ECHAM B2 2050s). Their findings are summarized in Table 3.2

Table 3. 2: Percentage change (from baseline) in flow and rainfall during wet season (June–September)

| GCMs             | % change in mean areal rainfall |              | % change in mean flow |              |
|------------------|---------------------------------|--------------|-----------------------|--------------|
|                  | 2050                            | 2080         | 2050                  | 2080         |
| SERS A2 Scenario |                                 |              |                       |              |
| CGCM2            | -1.1                            | <b>-10.5</b> | -12.5                 | <b>-46.6</b> |
| ECHAM            | 5.5                             | 12.4         | -1.3                  | -6.6         |
| HadCM3           | 1.6                             | 5.3          | -15.9                 | -24.4        |
| SERS B2 Scenario |                                 |              |                       |              |
| CGCM2            | -3.2                            | -6.3         | -43.4                 | -36.6        |
| ECHAM            | 13.1                            | <b>17.3</b>  | <b>12.4</b>           | -0.6         |
| HadCM3           | 2.5                             | 3.7          | -14.6                 | -27.5        |

Kim (2007) has also carried out climate change impact study on Upper Blue Nile River Basin using the out put of six GCM Models; CCSR,CGCM, CISRO,ECHAM4 ,GFDL , HADCM and SERS emission scenario A2. He weighted the output of the six models to find plausible climatic conditions for 2050s.

Based on the correlation matrix and the relative location of the station (this study) selected Deberemarkos station as a key or representative station for the whole basin, and generated monthly precipitation at this station using stochastic process. After generating monthly precipitation for this key station the monthly precipitation of the other stations was conditioned based on this station using the spatial CGM (conditional generation method).

This study has found different change in precipitation and temperature over the study area in all the six models and it adopted the weighted mean for impact assessment using water balance model. The findings are summarized in Table (3-3)

Table 3. 3 Changes in climatic variables and runoff for the 2050s

| GCM    | $\Delta P$ (%) | $\Delta T$ (°C) | $\Delta PET^a$ (%) | $\Delta Q^a$ (%) |
|--------|----------------|-----------------|--------------------|------------------|
| Weight | 11             | 2.3             | 16                 | 4                |
| CCSR   | 44             | 1.4             | 9                  | 80               |
| CGCM   | -3             | 1.7             | 11                 | -14              |
| CSIRO  | -11            | 2.1             | 14                 | -32              |
| ECHAM  | 33             | 2.4             | 17                 | 64               |
| GFDL   | 1              | 1.7             | 11                 | -13              |
| HADCM  | 6              | 2.6             | 19                 | -11              |

<sup>a</sup> PET and Q represent potential evapotranspiration and runoff, respectively.

Conway (2004) reported that with respect to the future climate in the Nile basin there is high confidence that temperatures will rise, leading to greater losses to evaporation. However, there is much less certainty about future rainfall because of the low convergence in climate model rainfall projections in the key headwater regions of the Nile. For example, Hulme et al. (2001) cited in(Conway, 2004) found large inter-model differences in the detail of rainfall changes over Ethiopia using results from seven recent climate model experiments. Inter-model disparities in future rainfall change over much of the basin are also presented in (IPCC, 2001).

“Some experts say there will be water increase with more rainfall from the Ethiopian plateau, and some say there will be a decrease because of water evaporation. No conclusion is yet made about the climate change impact on Nile water availability<sup>3</sup>.”

<sup>3</sup> <http://www.moew.gov.ae/min/index.jsp> (accessed March 22,2008)





## 4 Methodology

### 4.1 Meteorological Data

There are around ten meteorological stations in and around Beles sub- basin. Five of these stations are first classes, which measure all meteorological variables such as rainfall, temperature, sunshine hour, relative humidity, pan evaporation, wind speed and directions. Almost all the stations in the sub basin were established recently and have shorter records. Pawe station has relatively longer record from 1987 to 2003. Although Chagni and Manduara stations were established before Pawe both of the stations have record gaps from year1990-2000. The locations of the meteorological stations in and around Upper Beles sub-basin are shown figure 4.1. Time series plots of all the meteorological stations in and around Upper Main Beles sub-basin is also provided in Annex: C

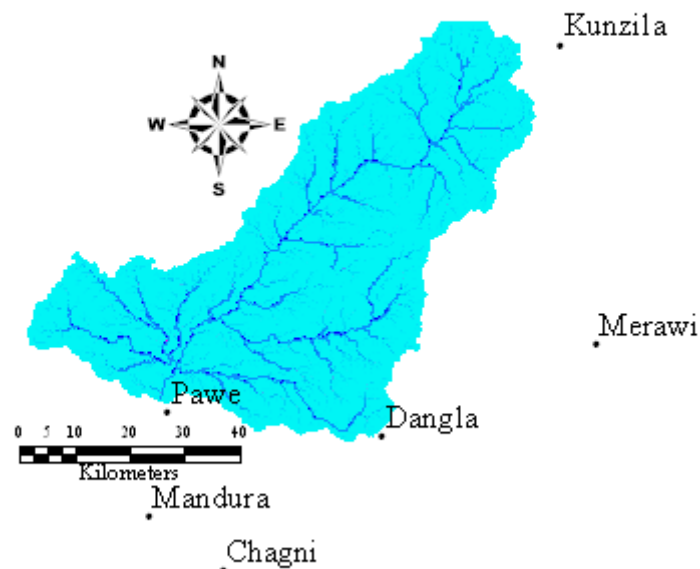


Figure 4. 1: Meteorological stations in and around Upper Beles Basin

## 4.2 Hydrological Data

There are two gauging station in the Beles sub- basin. The gauged part of the basin is about 30% of the total basin area (Figure 4.2). Flow data for Main Beles at bridge (3431 km<sup>2</sup>) since 1983 and Gilgel Beles flow near Mandura (675 km<sup>2</sup> ) since 1982 were collected from Ministry of Water Resource, department of hydrology. Time series plots of Main Beles flow data is provided in Annex: D.

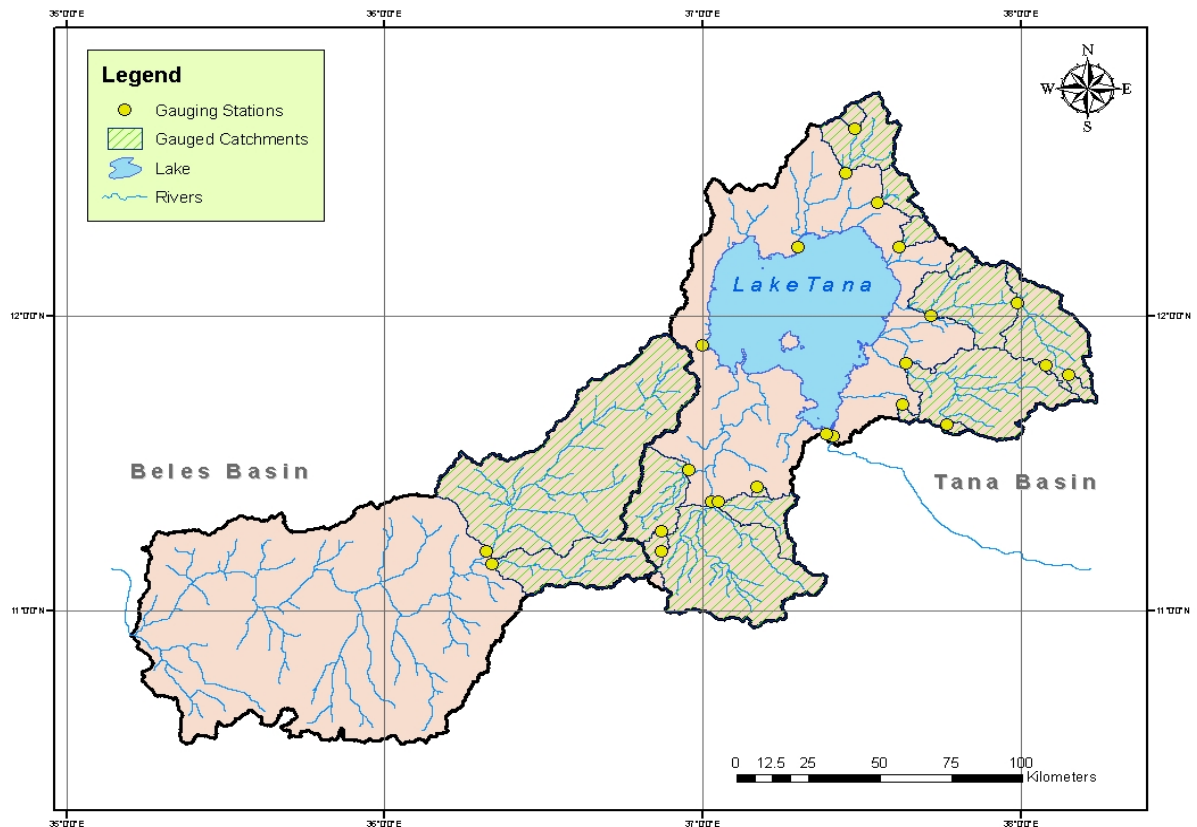


Figure 4. 2 Hydrological gauging stations in the Tana and Beles Basins (source SMEC)

## 4.3 Data screening

When simulating the hydrological system the data to be used should be stationary, consistent, and homogeneous (Dahmen and Hall, 1990). A time series of a hydrological data is stationary if its statistical properties such as mean, standard deviation and higher order moments are unaffected by the choice of time origin. Inconsistency is a change in the amount of systematic error associated with the recording data. It can arise from the use of different instruments and methods of observation. And non-homogeneity is a change in the statistical properties of the time

series. Its cause can be either natural or man made. These include alterations to land use, relocation of the observation stations and implementation of flow diversion

The four principal steps of data screening procedures given by (Dahmen and Hall, 1990) were adopted in this study:

- Rough screening of data and computation of monthly and annual totals for the hydrological year
- Plotting monthly and annual total and noting any trend or discontinuities.
- Testing the time series for absence of trend with Spearman's rank- correlation method
- Split record test: F-test for the stability of variance and t-test for stability of mean.

The completeness of data at each hydrological and metrological stations and observer's arithmetic when computing totals were checked, and monthly and annual totals were graphed in Excel. Any discontinuities were noted. The last two tests were conducted only for one station to identify existence of any trend which can be related to past climatic condition.

Tests for absence of trend with Spearman's rank correlation and F-test for stability of variance and t-test for the stability of mean were carried out using SPELL-Stat program. SPELL-Stat program is a simple and reliable time series analysis program developed to provide an easy way to evaluate homogeneity, consistency and independence of hydrological data (Gragne, 2007; Guzman and Librada, 2004)

#### **4.4 Weather generation**

Climate models are often combined with hydrological models for the purpose of simulating the effect of climate change on the stream flow of the river or on the water balance of the drainage basins in general. Normally long periods of daily weather data mainly rainfall, minimum and maximum temperature are required to study the long term impact of climate change on the watershed. But in many areas such data are either incomplete or records may not have sufficient length, which is the case in this study. Therefore, it is desirable to generate synthetic daily weather data to meet such needs.

Stochastic weather generators are numerical model which produces synthetic daily time series of climate variables such as precipitation, temperature and solar radiation with certain statistical properties(Semenov *et al.*, 1998b). Weather generators are now widely used by researchers from many different backgrounds in conjunction with their impact models. They are becoming a standard component of decision support systems in agriculture, hydrology and environmental management (Semenov and Barrow, 1997).

In this study two weather generator models, CLIMGEN, developed in USA and LARS-WG developed in Europe were tested for their applicability under limited data. Both models are belongs to public domain. The two models were compared based on the statistical measures such as mean difference and variance. The main objective here is to use relatively better weather generator model to fill the large gaps observed in the selected meteorological stations. The comparison was carried out on Mandura station which has rainfall and temperature records from 1980-1990 and the models relative ability to generate synthetic data from 1980-2001 were used for comparison. A review of each model is provided here under.

#### 4.4.1 ClimGen weather generator

ClimGen is a daily time step stochastic model that generates daily precipitation, minimum and maximum temperature, solar radiation, humidity and wind speed data series with similar statistics to those of the historical weather data. ClimGen is developed by Gaylon S.Campell(Washington State University,1990). It is modified version of WGEN model which is the most extensively applied Weather Generator Model in United States developed by Richardson & Wright (1984). ClimGen is a public domain model<sup>4</sup>.

ClimGen uses a Weibull distribution to generate precipitation amounts instead of the Gamma distribution used by WGEN. Weibull distribution is easier to parameterize, describes well the distribution of precipitation amounts, and can be simplified for applications to conditions with minimum data<sup>3</sup>. Selker and Haith (1990) cited in(Tingem *et al.*, 2007) also showed the Weibull distribution to be superior to other probability distribution of daily precipitation amount. ClimGen model requires inputs of daily series of precipitation, minimum and maximum temperature, solar radiation, humidity and wind speed data to calculate parameters used in the generation process for any length of period at a location of interest (Tingem *et al.*, 2007).

The technique used in ClimGen for generating maximum and minimum temperature is based on the assumption that temperature is a weakly stationary process. This approach considers maximum and minimum temperature to be a continuous multi-variate stochastic process with daily means and standard deviations conditioned by the precipitation status (wet or dry) of the day. ClimGen uses quadratic spline functions to produce daily values for monthly-calculated quantities of mean weather variables chosen to ensure that the averages of the daily values are continuous across month boundaries, and that the first derivative of the function is continuous across month boundaries.<sup>5</sup>

---

<sup>4</sup> <http://www.bsyse.wsu.edu/climgen/>

<sup>5</sup> (<http://www.bsyse.wsu.edu/climgen/>, accessed Jan 2008)

ClimGen weather generator model requires at least 10 years of temperature data for good temperature generation and at least 25 years of data, so as to get a good spread of precipitation. However there is no formal constraint, .ClimGen can work with as little as 1 year, but may not be possible to get proper variation.

The observed daily data of rainfall and maximum temperature of Mandura station, for the data period 1980-1990(10 years) were prepared in the Universal Environmental Database (UED) and used as input for generating the location parameter file. The location parameter file contains monthly statistics which are used for generating synthetic climate variables for desired period

#### **4.4.2 LARS-WG stochastic weather generator**

LARS-WG is a stochastic weather generator developed by Dr. Mikhail Semenov of Rothamsted Research, UK. It is a public domain model<sup>6</sup> It generates a suite of climate variables, namely, precipitation, maximum and minimum temperature and solar radiation (Semenov and Barrow, 1997). Precipitation in this case is considered as the primary variable and the other three variables on a given day are conditioned on whether the day is wet or dry . The simulation of precipitation occurrence is based on distributions of the length of continuous sequences, or series, of wet and dry days.

It utilizes semi-empirical distributions for the lengths of wet and dry day series, daily precipitation and daily solar radiation. The semi-empirical distribution  $Emp = \{a_0, a_i; h_i, i=1, \dots, 10\}$  is a histogram with ten intervals,  $[a_{i-1}, a_i)$ , where  $a_{i-1} < a_i$ , and  $h_i$  denotes the number of events from the observed data in the  $i$ -th interval. Random values from the semi-empirical distributions are chosen by first selecting one of the intervals (using the proportion of events in each interval as the selection probability), and then selecting a value within that interval from the uniform distribution. Such a distribution is flexible and can approximate a wide variety of shapes by adjusting the intervals  $[a_{i-1}, a_i]$ (Semenov *et al.*, 1998a)

---

<sup>6</sup> <http://www.rothamsted.bbsrc.ac.uk/mas-models/larswg.php>

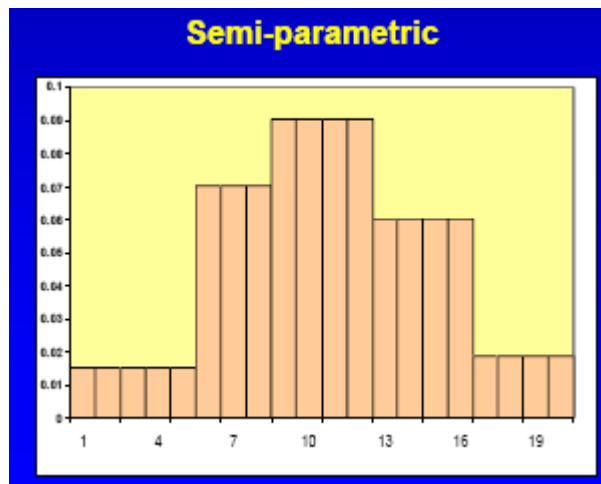


Figure 4. 3 Semi-empirical distribution used by LARS-WG (histogram)

The simulation of precipitation occurrence is modelled as alternate wet and dry series, where a wet day is defined to be a day with precipitation  $>0$  mm. The length of each series is chosen randomly from the wet or dry semi-empirical distribution for the month in which the series starts. In determining the distributions, observed series are also allocated to the month in which they start. For a wet day, the precipitation value is generated from the semi-empirical precipitation distribution for the particular month independently of the length of the wet series or the amount of precipitation on previous days<sup>7</sup>

The first step for generating daily time series of data in the LARS-WG models is SITE ANALYSIS. This step is called calibration. The calibration process results in a parameter file containing information about the statistical characteristics of the observed data, which is then used to generate series of synthetic data. Model verification is generally undertaken by comparing the statistics of the synthetic data with those of the observed data set used to calibrate the model. One known problem with this types of weather generator is that it tends to underestimate the variability of observed time series - this is due to the way in which the different climate variables are modelled, e.g., Fourier series are used to smooth the statistical characteristics (i.e., the means and standard deviations) of the non-precipitation climate variables on wet and dry days and so immediately a reduction in variability is introduced<sup>8</sup>.

<sup>7</sup> <http://www.rothamsted.bbsrc.ac.uk/mas-models/larswg/download.php>

<sup>8</sup> <http://www.cics.uvic.ca/scenarios/index.cgi> accessed on Jan 26, 2008)

## 4.5 General circulation Model (GCM)

Among the wide range of GCM models HadCM3 (Hadley Centre for Climate prediction and Research, England), ECHAM4 (Max Plank Institute, Hamburg, Germany), CGCM2 (Canadian Centre of Climate Modelling and Analysis), GFDL\_R30 (Geophysical Fluid Dynamics Laboratory & NOAA), CSCR (Centre for climate Systems Research & Japanese National Institute for Environmental studies), CSIRO (Australian Commonwealth Scientific and Industrial Research organization are commonly used in various studies. GCM models account for the most important physical processes; in some cases chemical and biological processes are also represented (Richard Jones *et al.*, 2004)..

As discussed in the previous section although it is recommended to use the Ensemble of different GCM model output to minimize the uncertainties, in this study , because of limitations of time we used the out put of only one GCM model namely: HadCM3.

HadCM3 (Hadley Centre Coupled Model version3) coupled atmosphere-ocean general circulation model is developed at the Hadley Centre in the UK. .It is a three-dimensional climate models, composed of two components the atmospheric model (HadAM3) and the ocean model (HadOM3), which includes a sea ice model. The atmospheric part of the model has a grid of  $2.5^{\circ}$  latitude and  $3.75^{\circ}$  longitude (i.e. gives a resolution of approximately 300km) and has 19 vertical levels. The ocean model has 20 vertical levels and a grid size of  $1.25^{\circ}$  latitude x  $1.25^{\circ}$  longitudes. Thus there are six ocean grids for every atmospheric one. In all, there are about a million grid points in the model. At each of these grid points in the atmosphere and ocean, equations are solved which describe the large scale balance of momentum, heat and moisture. This places a strain on the resources of even the largest and fastest computer<sup>9</sup>

The main reason for the selection of this model for impact study is that the model output is available together with the downscaling tool<sup>10</sup>. The model result is available for the A2 and B2 scenarios, where A2 is referred as the medium-high emissions scenario and B2 as medium-low emission scenario. For the two of these emission scenarios three ensemble members(a, b, and c) are available where each refer to different initial point of climate perturbation along the control run Hanson et al,2004 cited in (Lijalem, 2006)

Currently data for ensemble 'a' only are available at the Canadian climate research centre therefore only A2a and B2a scenarios were considered in this study.

---

<sup>9</sup> <http://www.metoffice.gov.uk/research/hadleycentre/models/modeldata.html>

<sup>10</sup> <http://www.cics.uvic.ca/scenarios/sdsm/select.cgi>

## 4.6 Downscaling

Among the widely applied statistical downscaling techniques the multiple linear regressions based model called SDSM and time lagged feed forward neural networks (TLFN) are used in this study. These techniques are briefly reviewed hereunder for the purpose of clarity and discussions that follow.

### 4.6.1 Statistical Downscaling Model (SDSM)

Statistical Downscaling Model is a hybrid of multiple linear regression and stochastic downscaling model developed by Rob Wilby and Christian Dawson in the UK. It is freely available decision support tool for assessing local climate change impact using a robust statistical downscaling technique<sup>11</sup>.

SDSM is best described as a hybrid of the stochastic weather generator and regression-based methods, because large-scale daily circulation patterns and atmospheric moisture variables are used to condition local-scale weather generator parameters at individual sites. The stochastic component of SDSM enables generation of multiple simulations with slightly different time series attributes, but the same overall statistical properties(Wilby and Harris, 2006)

The spatial downscaling of daily predictor-predictand relationships in SDSM is done by using multiple linear regression techniques. SDSM reduces the task of statistical downscaling daily weather series into a number of discrete processes such as (1) screening of potential predictor variable (2) Calibration of the model to determine model parameters (3) weather generation, generating ensemble of synthetic daily weather series given the selected predictor variables. (4) Generation of ensembles of future data using GCM-derived predictor variables corresponding to future climate scenarios (5) Analysis of observed and downscaled data based on their statistical characteristics for easy comparison.

The two frequently used terms in statistical downscaling are defined as follows as used in many publications;

The *predictor* is the input data used in statistical models, typically a large scale variable describing the circulation regime over a region. The predictor is also known as 'independent variable', or simply as the 'input variable', usually written as

$$Predictand = f(\text{predictors})$$

The *predictand* is the output data, typically the small-scale variable representing the temperature or rainfall at a weather/climate station. The *predictand*, is also known as 'dependent variable', 'response variable', 'responding variable', 'regressand', or simply as the 'output'

---

<sup>11</sup> <https://co-public.lboro.ac.uk/cocwd/SDSM/index.html>



#### 4.6.1.1 Statistical Downscaling Model inputs

Predictor data files for SDSM model were downloaded from the Canadian Institute for climate studies (CICS) website.<sup>12</sup> The predictor variables for HadCM3 were provided on a grid box by grid box basis of size 2.5° latitude and 3.75° longitude (Figure 4.4). The watershed area of Beles basin lies in two grid boxes (10° latitude and 37.5° longitude and 12.5° latitude and 37.5° longitude).

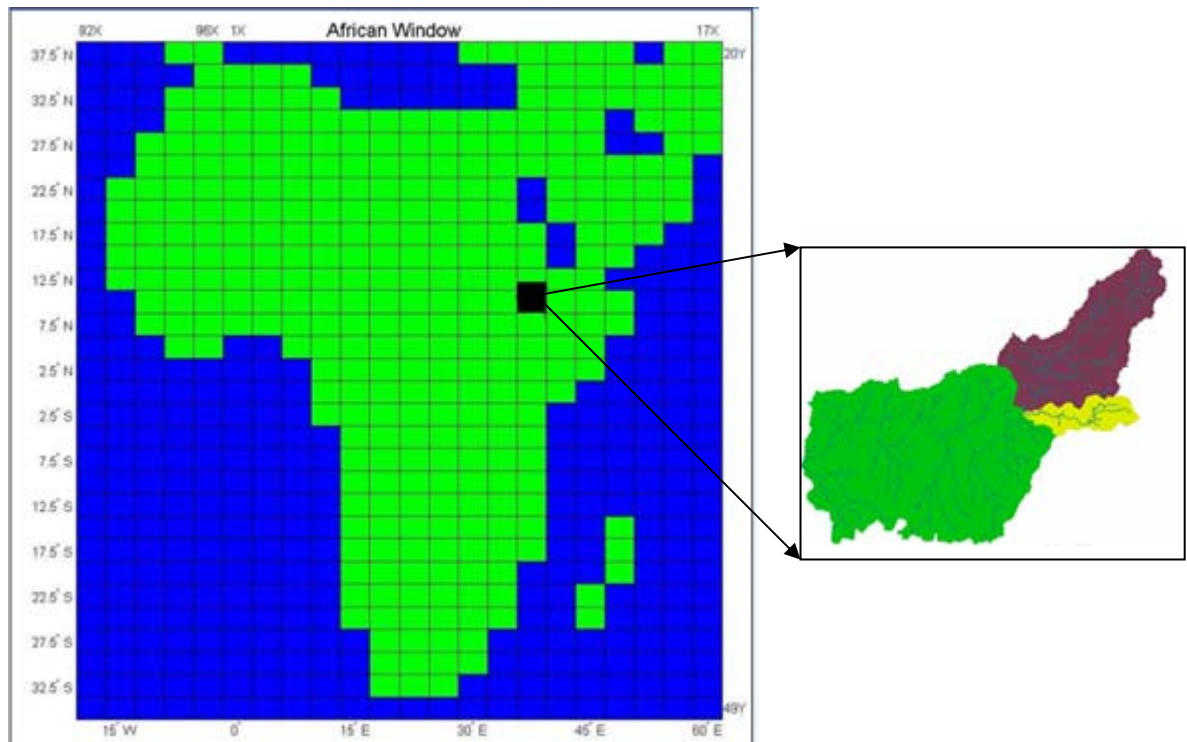


Figure 4. 4: African continent Windows with 2.5° latitude x 3.75° Longitude from which grid of study area selected shown in black square box

The predictor data files downloaded from the grid of interest consists of the following three directories:

NCEP\_1961-2001: This directory contains 41 years of daily observed predictor data, derived from the NCEP reanalysis, normalized over the complete 1961-1990 period. These data were interpolated to the same grid as HadCM3 (2.5 latitude x 3.75 longitude) before the normalization was implemented.

H3A2a\_1961-2099: This directory contains 139 years of daily GCM predictor data, derived from the HadCM3 A2 (a) experiment, normalized over the 1961-1990 period.

H3B2a\_1961-2099: This directory contains 139 years of daily GCM predictor data, derived from the HadCM3 B2 (a) experiment, normalized over the 1961-1990 period.

<sup>12</sup> <http://www.cics.uvic.ca/scenarios/sdsm/select.cgi>

NCEP data are re-analysis data sets from the National Center for Environmental Prediction, and re-gridded to conform to the grid system of HadCM3.

Reanalysis data are fine resolution gridded data which combine observations with simulated data from numerical models, through a process known as data assimilation. The observations, along with data from satellites and information from previous model forecast are input into a short-range weather forecast model. This is integrated forward by one time step (typically 6 hours) and combined with observational data for corresponding period. The result is a comprehensive and dynamically consistent three-dimensional gridded data set (the analysis) which represents the best estimate of the atmosphere at that time (IPCC-TGCI, 1999).

Table 4. 1: List of Predictor variables derived from African window for the grid on the study area (Twenty six predictor variables)

| Predictor variable | Description                 | Predictor variable | Description                    |
|--------------------|-----------------------------|--------------------|--------------------------------|
| mslpaf             | mean sea level pressure     | p5_Zhaf            | 500hpa divergence              |
| p_faf              | surface air flow strength   | p8_faf             | 850hpa airflow strength        |
| p_uaf              | surface zonal velocity      | p8_uaf             | 850hpa zonal velocity          |
| p_vaf              | surface meridional velocity | p8_vaf             | 850 hpa meridional velocity    |
| p_zaf              | surface vorticity           | p_zaf              | 850 hpa vorticity              |
| p_thaf             | surface wind direction      | p850af             | 850hpa geopotential height     |
| p_zhaf             | surface divergence          | p8thaf             | 850hpa wind direction          |
| p5_faf             | 500hpa air flow strength    | p8zhaf             | 850 hpa divergence             |
| p5_uaf             | 500hpa zonal velocity       | r500af             | relative humidity at 500 hpa   |
| p5_vaf             | 500hpa meridional velocity  | r850af             | relative humidity at 850 hpa   |
| p5_zaf             | 500hpa vorticity            | rhumaf             | near surface relative humidity |
| p500af             | 500hpa geopotential height  | shumaf             | surface specific humidity      |
| p5thaf             | 500hpa wind direction       | tempaf             | mean temperature at 2 m        |

All predictors, with the exception of wind direction, have been normalized with respect to the 1961-1990 mean and standard deviation

#### 4.6.1.2 Predictor variables selection

The choice of predictor variable(s) is one of the most challenging stages in the development of any statistical downscaling model because the decision largely determines the character of the downscaled scenario. The decision process is also complicated by the fact that the explanatory power of individual predictor variables varies both spatially and temporally (Hessami *et al.*, 2007; Wilby and Dawson, 2007).

Observed daily data of large scale predictor variables representing the current climate condition (1961-2001) derived from the NCEP reanalysis data set were used to investigate the percentage of variance explained by each predictor-predictor pairs.

The SDSM model has the option to specify whether the predictand-predictor relationship is governed by the intermediate process or not. In case of daily temperature where the predictand-predictor process is not regulated by intermediate process unconditional process was used, whereas for daily precipitation where the amounts depend on wet-day occurrence the conditional process was chosen. Also the significant level which is used for testing the significance of predictor-predictand correlation was set to the default value of ( $p < 0.05$ ). Since the temporal strength of predictor variables varies month by month, the most appropriate combination of predictors was chosen by looking at the analysis output of all the twelve months. The inter-variable correlations were investigated using the correlation matrix and the partial correlations between the selected predictors and predictand were used to identify the amount of explanatory power that is unique to each predictor.

The scatter plot functionality of the SDSM model was also used for visual inspection of inter-variable behavior, which indicates the nature of association whether or not data transformation is needed and the importance of outliers

Predictors have to be chosen on the balance of their relevance to the target predictand and their accurate representation by climate mode (Wilby and Wigley, 2000, Wilby et al, 2004) cited in (Hessami *et al.*, 2007). Hessami et al (2007) have also mentioned that when modeling precipitation, the most commonly used predictor variables were relative and specific humidity at 500hpa, surface airflow strength, 850hpa zonal velocity and 500hpa geopotential height. And for modeling temperature, mean sea level pressure, surface vorticity and 850hpa geopotential height were the most dominant variables.

#### **4.6.1.3 Model calibration**

Model calibration was carried out based on the selected predictor variables that are derived from the NCEP data set. Model calibration in this case is finding the coefficients of the multiple linear regression equation parameters that relate large scale atmospheric variables derived from NCEP and local scale variables (observed Temp and precipitation).

The temporal resolution of the downscaling model for precipitation was specified as seasonal for Pawe precipitation downscaling station whereas monthly for Dangila and Bhardr stations. In monthly models different model parameters are used for each month where as in seasonal models all months of the same season will have the same model parameter. Seasonal model can be used in situations where data are too sparse at the monthly level for model calibrations, for example in a low incidences of precipitation in semi arid area (Wilby and Dawson, 2007). From the fifteen years of data representing the current climate condition the first ten years (1987-1996) were considered for calibrating the regression models.

#### **4.6.1.4 Weather Generator and Validation**

Ensembles of synthetic daily weather series were produced using the atmospheric predictor variables derived from the NCEP re-analysis data set and regression model weights produced during calibration. This enables the verification of calibrated model as well as the synthesis of artificial time series representative of present climate condition. Individual ensemble members are considered equally plausible local climate scenarios realized by a common set of regional-scale predictors. (Wilby and Dawson, 2007) noted that local temperatures are largely determined by regional forcing and the difference between the ensemble members is minimal whereas precipitation series display more “noise” arising from the local factors and show larger differences between individual ensemble members.

#### **4.6.1.5 Scenario Generation**

In this case twenty ensembles of synthetic daily weather series were produced based on the atmospheric predictor variables derived from HadCM3 GCM model (emission scenarios A2a and B2a) and regression model weights produced during the calibration process. This is based on the assumption that the predictor-predicand relationships under the current condition remain valid for future climate conditions.

#### **4.6.2 Artificial Neural Networks**

An ANN is composed of set of simple processing nodes, each of which receives inputs from other nodes and outputs value to further nodes. The resultant net of nodes will have some nodes dedicated to receiving primary inputs, and some to providing final output from the overall net. Each node is connected to others via weighted links, and calculates a sum of the weighted inputs. This sum is then transformed by some function that may be either linear or non linear such as sigmoid, which becomes the node output value. Nodes are generally arranged in layers, with an input layer connected to a hidden layer which is in turn connected to output layer. An ANN-MLP model is usually made up of a number of layers of processing elements (neurons) with multiple connections between the elements of each layer (Wilby *et al.*, 1998)

The architecture of artificial neural networks is versatile enough to describe wide range of relationships between geophysical variables. Particularly, an appropriate topology of the neural network can satisfactorily represent a non-linear association that could not be explained by explicit mathematical formulations. Among the various types of topologies, a multi-layer feed-forward neural network has received considerable attention due to its ability and efficiency in approximating physical relationships. The layer of neural networks consists of nodes that have similar order of connecting links before and/or after the processing node. The computations across

layers proceed in one direction and are not reversible. That is why the term ‘feed-forward’ is coined in the name of the network architecture.

Although feed-forward neural networks are popular in many application areas, they are not well suited for temporal sequences processing due to the lack of time delay and/or feedback connections necessary to provide a dynamic model. Time lagged feed-forward networks (TLFN) and recurrent networks (RNN) are the two major groups of dynamic neural networks mostly used in time series analysis. However, the latter require complex training algorithms and hence are computationally costly (Dibike and Coulibaly, 2006). Therefore in this study the time-lagged feed forward Neural Network (TLFN) were used for downscaling daily precipitation amount and minimum and maximum temperatures.

### Time-Lagged feed forward Neural Network (TLFN)

A time-lagged feed-forward neural network (TLFN) is a neural network that can be formulated by replacing the neurons in the input layer of a MLP with a memory structure, which is sometimes called a tap delay line. The size of the memory layer (the tap delay) depends on the number of past samples that are needed to describe the input characteristics in time and must be determined on a case-by-case basis. A TLFN uses delay-line processing elements which implement memory by simply holding past samples of the input signal as shown in Fig 4.5. Given an input signal consisting of the present value  $x(n)$  and the  $p$  past values  $x(n - 1), \dots, x(n - p)$  stored in a delay line memory of order  $p$ , the free parameters of the network are adjusted to minimize the mean-squared error between the output of the network and the desired (or target) response. Detail descriptions are given (Dibike and Coulibaly, 2006; Muluye and Coulibaly, 2007)

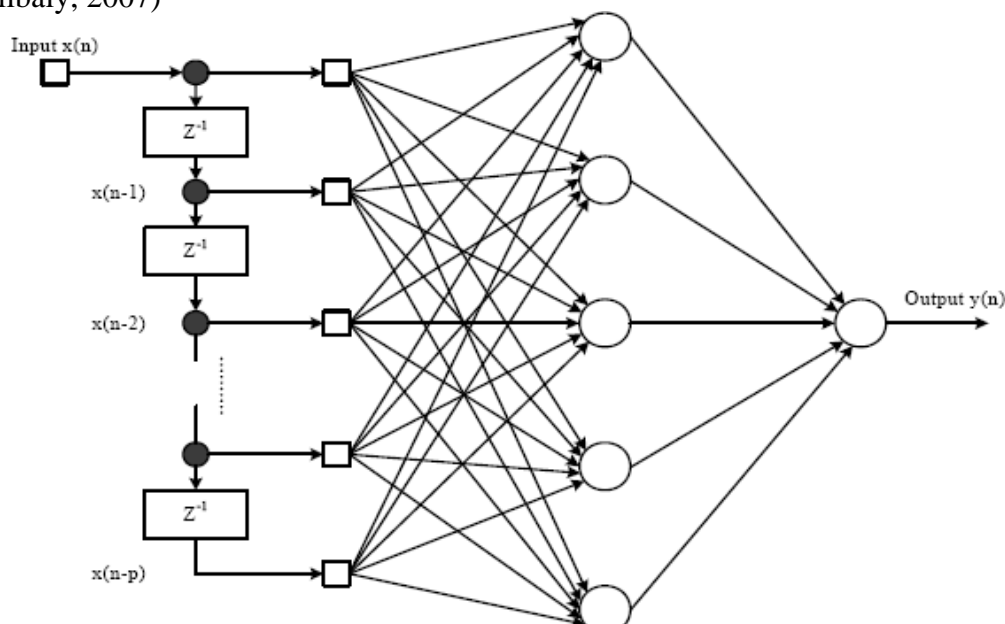


Figure 4. 5: Time-lagged feed-forward network (TLFN) adopted from (Muluye and Coulibaly, 2007).

## **4.7 HEC-HMS Hydrological Model**

HEC-HMS is a comprehensive hydrologic model developed by Hydrologic Engineering Center (HEC) of United States Army Corps of Engineers (USACE). It is designed to simulate the precipitation-runoff processes of dendritic watershed systems. It is also designed to be applicable in a wide range of geographic areas for solving the widest possible range of problems. This includes large river basin water supply and flood hydrology, and small urban or natural watershed runoff. Hydrographs produced by the program are used directly or in conjunction with other software for studies of water availability, urban drainage, flow forecasting, future urbanization impact, reservoir spillway design, flood damage reduction, floodplain regulation, wetlands hydrology (HEC, 2006b)

The main reasons for the selection of HEC-HMS hydrological model is that the model is physically based, spatially distributed and it belongs to public domain. It has been used in wide geographical area including climate change studies. Bashar and Zaki(2005) have applied this model for the whole Upper Blue Nile Basin and they have found good performance.

The current version of HEC-HMS (3.1.0) is a highly flexible package. It includes different methods to simulate infiltration losses, transforming excess precipitation, baseflow estimation and channel routing. For this particular study, SMA model, Clark's unit hydrograph and Muskingum method were used. Details are given in subsequent sections:

### **4.3.1 Continuous soil moisture accounting (SMA) model**

SMA method allows for long-term continuous simulation of hydrologic processes that occur and change over time in a watershed. This is achieved by simulating the movement of precipitation through storage volumes that represent canopy interception, surface depressions, the soil profile and two groundwater layers. Computational components of this algorithm also include evapotranspiration (ET), surface runoff, and groundwater flow (HEC, 2006b).

Conceptually, the HMS SMA algorithm divides the potential path of rainfall on to a watershed in to five layers as shown in Figure 4.6. Besides precipitation the only other input to SMA algorithm is potential evapotranspiration rate. For the simulation of water movement through the various storage zones, the maximum capacity

(maximum depth) of each storage zone, initial storage condition in terms of percentage of the filled portion of each zone, and the transfer rates, such as the maximum infiltration rate, need to be specified

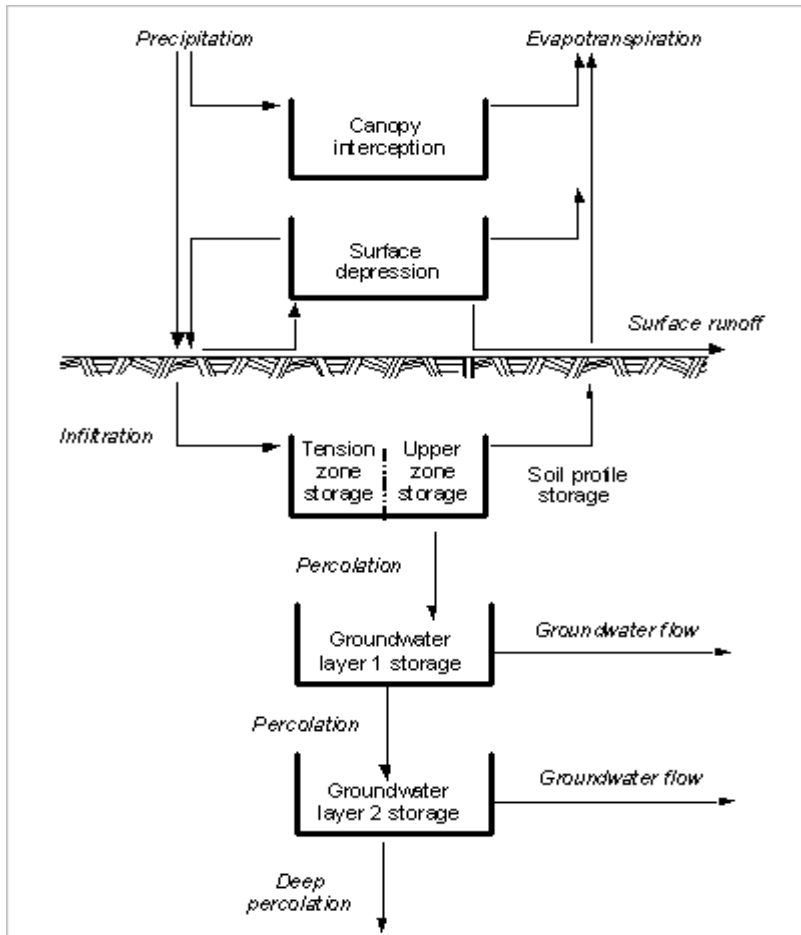


Figure 4. 6: Conceptual schematic of the continuous soil moisture accounting algorithm (Bennett, 1998) (source *HEC-HMS Technical manual*)

### 4.3.2 Clark Unit Hydrograph Transform

Clark unit hydrograph technique was used to transform the excess rainfall to direct runoff. In this method, the processes of translation and attenuation of excess rainfall dominate the movement of flow through a watershed. Translation is the movement of flow down gradient through the watershed in response to gravity whereas attenuation is a reduction of the magnitude of the discharge as the excess is stored throughout the watershed. The time area curve built in the model develops the translation hydrograph resulting from a burst of precipitation, and the resulting translation hydrograph is routed through a linear reservoir for accounting storage attenuation affects across the sub basins.

Time of concentration and storage coefficient are the two important parameters in Clark unit hydrograph transforming excess rainfall in to runoff. The time of concentration is used in the development of the translation hydrograph where as storage coefficient is used in the linear reservoir that accounts for storage change.

#### **4.3.3 Linear Reservoir Model**

The linear-reservoir base flow model is used in conjunction with the continuous soil-moisture accounting (SMA) model and best calibrated using procedures consistent with those used to calibrate that model (HEC, 2006b). It uses a linear reservoir to model the recession of base flow after event. The total baseflow is the total outflow from two ground water layers. The initial base flow at the beginning of the simulation and the groundwater storage coefficient for the two layers were determined by calibration. To assist the calibration process base flow separation was carried out using Soil and Water Assessment Tool (SWAT) base flow separator program.

The base flow separation using SWAT baseflow separator program based on the daily flow data recorded at main Beles Bridge shows that about 60% of the flow is contributed by the base flow and the rest from surface runoff. The base flow recession constant (alpha factor), which is the rate at which ground water is returned to stream is found to be 0.02 and the base flow days ,the number of days for the base flow recession to decline through one long cycle has been found to be about 114 days.

#### **4.3.4 Muskingum Model**

The Muskingum routing method uses simple conservation of mass approach to route flow through the stream reach. The travel time of a flood wave passing through the reach (k) and the measure of degree of storage(x) need to be determined through calibration

#### **4.3.5 HEC-HMS Model setup**

HEC-HMS has four main model components: basin model, meteorologic model, control specifications and input data (time series, paired data and gridded data). The Basin Model, for instance, contains information relevant to the physical attributes of the model, such as basin areas, river reach connectivity, or reservoir data. Likewise, the Meteorological Model holds rainfall data. The Control Specifications section contains information pertinent to the timing of the model such as when a storm occurred and what type of time interval is to be used in the model, etc. Finally, the input data component stores parameters and boundary conditions for basin and meteorologic models (HEC, 2006b). Each of the sections is explored below individually



#### 4.3.6 Basin Model

The Basin model contains the hydrologic element and their connectivity that represents the movement of water through the drainage system. Its main purpose is to convert the atmospheric conditions in to stream flow at specific locations in the watershed(HEC, 2006b). HEC-GeoHMS, an Arc view extension developed by the U.S.Army Corps of Engineers (USACE) was employed to create the basin model background map file and to delineate the sub catchments from the Digital Elevation Model (DEM). DEM was downloaded from the Consortium for Spatial Information (CGIAR\_CSI)<sup>13</sup>, which provides the NASA Shuttle Radar Topographic Mission (SRTM) 90 m x 90 m resolution Digital Elevation Data for the entire world. The physical characteristics of the stream such as length, upstream and downstream elevations and slope as well as sub basin physical characteristics such as longest flow lengths, centeroidal flow length and slopes derived from DEM were used for estimating hydrologic parameters. Longest flow path information for example was used for estimating time of concentration

The background maps provide a spatial context for the hydrologic elements composing basin model. The maps are not actually used in the computational process, but they can be very helpful in showing the spatial relationship between the elements. They are commonly used for showing the boundaries of a watershed or the location of streams. Terrain preprocessing, Basin processing and HMS model support are the main functionalities of HEC-GeoHMS. In the terrain preprocessing DEM derived from SRTM is used as input and a series of steps consisting of computing the flow direction, flow accumulation, stream definition, stream delineation, watershed delineation, and watershed aggregation were performed step by step to derive the drainage networks. The basin processing step gives capability of merging, editing and subdividing of basins and rivers whereas the HMS model support produces a number of hydrologic inputs that are used directly in HMS.

With this the basin model and background map files are included and imported in to HMS the setup is then completed with meteorologic and control specification.

As it can be seen in Figure 4.7 the Upper main Beles sub-basin is divided in the three small sub-basins. The main purpose is to make the hydrologic model semi distributed

---

<sup>13</sup> . <http://www.ambiotek.com/srtm>

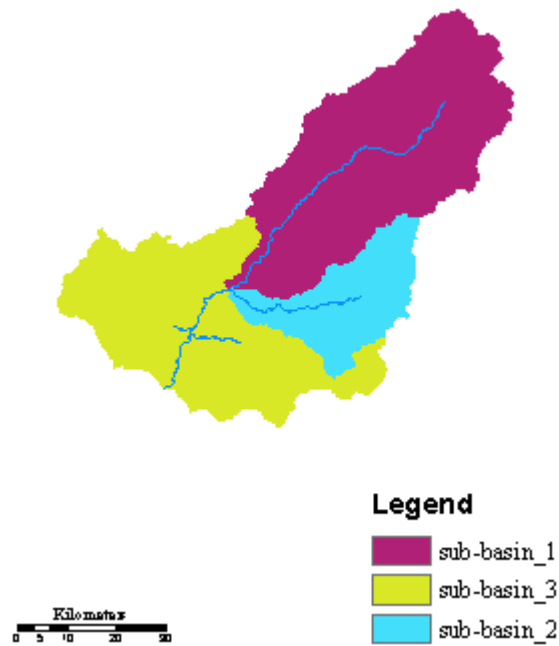


Figure 4. 7: The three small sub-basins of Upper Main Beles

#### 4.3.7 Meteorologic Model

The meteorologic component is the first computational element by means of which precipitation input is spatially and temporally distributed over the river basin. The spatio-temporal precipitation distribution is accomplished by the gauge weight method. The Thiessen polygon technique was used to determine the gauge weights (Figure 4.8). The Meteorologic model uses monthly evapotranspiration as input for continuous hydrological simulation which is the case for this model. For this particular study potential evapotranspiration computation were carried out using FAO Penman- Monteith method in Cropwat model. FAO Penman-Monteith Method is recommended as a sole standard method for the definition and computation of the reference evapotranspiration (ET<sub>o</sub>)(Allen *et al.*, 1990) It requires radiation, min and max temperature, air humidity, and wind speed as input.



Figure 4. 8 : Thiession polygon for Upper main Beles sub-basin

#### 4.3.7.1 Control specification and HEC-DSSVue

Control specifications are one of the main components of a project, and principally used to control simulation runs. They control when a simulation starts and stops, and what time interval is used in the simulation. A simulation run is created by combining a basin model, meteorologic model, and control specifications.

HEC-DSS is a database system designed by U.S.Army Corps of Engineers for efficient storage and retrieval of data that is typically sequential (HEC, 2006a). HEC-DSS uses a block of sequential data as the basic unit of storage which results in a more efficient access of time series or other sequentially related data. Data is stored in blocks, or records within a file and each record is identified by a unique name called path name.

For efficient manageability rainfall and discharge time series were stored in HEC-DSSVue(Hydrologic Engineering Center Data Storage System Visual Utility Engine) and imported to HMS.



## 5 Results and discussions

### 5.5 Data Analysis

Due to inaccessibility, remoteness and economical limitations the Beles sub basin has very sparse observational networks and some of the stations have large data gap (see Annex: A and C), while others have short record length. Therefore an attempt has been made to generate synthetic daily weather data to fill the data gaps observed. The results are presented in the following sections:

#### 5.1.1 Data Screening

Rainfall data screening for the five stations in the study area were carried out through visual inspection of daily data and arithmetic checks on the monthly totals. Because of long data gaps and short records Mandura and Kunzila stations were not used in this study. Only three of the stations which have relatively good data were considered for catchment modelling and impact assessment. The relationship between the selected stations was explored using correlation matrix shown in Table 5.1

Table 5. 1: Correlation matrix of the three meteorological stations using daily, Monthly and Long-term daily average rainfall records and maximum temperature

|                                      | Bhardar | Dangila | Pawe |
|--------------------------------------|---------|---------|------|
| Daily rainfall records (1997-2004)   |         |         |      |
| Bhardar                              | 1       |         |      |
| Dangila                              | 0.39    | 1       |      |
| Pawe                                 | 0.33    | 0.42    | 1    |
| Daily longterm average (1987-2001)   |         |         |      |
| Bhardar                              | 1       |         |      |
| Dangila                              | 0.82    | 1       |      |
| Pawe                                 | 0.83    | 0.84    | 1    |
| Monthly rainfall records (1997-2004) |         |         |      |
| Bhardar                              | 1       |         |      |
| Dangila                              | 0.89    | 1       |      |
| Pawe                                 | 0.88    | 0.93    | 1    |
| Daily maximum temp(1998-2002)        |         |         |      |
| Bhardar                              | 1       |         |      |
| Dangila                              | 0.83    | 1       |      |
| Pawe                                 | 0.8     | 0.9     | 1    |

As it can be seen from the above tables the correlation matrix between the stations on the monthly and long-term daily average basis shows well agreement. In both cases the rainfall amount of Pawe station shows quite well agreement with the other two stations. The agreement is also acceptable on the daily basis. Pawe station also shows good agreement in daily max temperature. Hence Pawe station can be taken as a representative of the climate stations in the basin.

### 5.1.2 Weather generation

The usual way of filling missing data is to use the data of the near by station either using regression analysis or spatial interpolation. The non overlapping data series between the stations hinders the use of regression analysis method to fill the missing data (Annex: B). some of the stations in the basin were established recently and have short records. On the other hand the reanalysis large scale predictor variables derived from NCEP don't include predictor variables after the year 2001. That means the data record after year 2001 will not be used for downscaling. This is one of the main constraints that led to the use of the weather generator model to fill in the missing data.

In this study ClimGen and LARS-WG models ability to generate rainfall time series under limited data were compared. The daily rainfall and maximum temperature data of Mandura station (1980-1990) were used as input for each model and twenty years of synthetic data (1980-2001) were generated. Model comparisons are made based on the monthly statistics such as mean difference and variance. As it can be seen in table (5.2 & 5.3) the departure of the simulated mean from the observed mean is very large in case of LARS-WG and small in ClimGen. The difference is mainly from the methods that each model is using to generate rainfall time series. LARS-WG model uses semi-empirical methods where as ClimGen uses the Weibul distribution. While ClimGen generates relatively better rainfall time series than LARS-WG model, the two models are equally good in generating maximum temperature. Therefore we have used ClimGen model to fill the data gaps observed in selected stations. The comparison plot of observed and simulated rainfall time series using ClimGen is shown in figure 5.1.

Table 5. 2: Output data from the statistical tests, showing the comparison of the observed rainfall, & maximum temperature monthly means and variances with those of 20 years of synthetic data generated by LARS-WG for Mandura station.

|                 | Jan  | Feb  | Mar   | Apr   | May   | Jun    | Jul    | Aug  | Sep   | Oct   | Nov | Dec  |
|-----------------|------|------|-------|-------|-------|--------|--------|------|-------|-------|-----|------|
| <b>Rainfall</b> |      |      |       |       |       |        |        |      |       |       |     |      |
| obs.mean        | 2.3  | 1.8  | 20.9  | 31    | 128.2 | 310    | 527.3  | 512  | 321.7 | 127.1 | 3.6 | 1.4  |
| obs.variance    | 3.94 | 6.12 | 37.93 | 47.61 | 72.35 | 118.57 | 274.37 | 271  | 143.9 | 72.62 | 8.3 | 3.58 |
| Sim mean        | 6.9  | 11.1 | 57.2  | 97.1  | 479.2 | 907.9  | 2484.8 | 2849 | 2577  | 872.6 | 57  | 110  |
| Sim.variance    | 10.2 | 16.3 | 69.94 | 150.5 | 471.7 | 543.08 | 409.5  | 232  | 376.1 | 342.8 | 40  | 39.3 |
| <b>Max Temp</b> |      |      |       |       |       |        |        |      |       |       |     |      |
| obs.mean        | 31.5 | 33   | 34.9  | 34.7  | 32.2  | 28.6   | 26.6   | 26.3 | 26.6  | 28.2  | 30  | 30.8 |
| obs.variance    | 2.27 | 2.6  | 1.9   | 2.5   | 3.48  | 1.99   | 1.67   | 1.23 | 1.53  | 0.8   | 1.6 | 1.76 |
| Sim mean        | 31.8 | 33   | 34.8  | 35.5  | 32.5  | 29.1   | 26.5   | 25.6 | 27.1  | 28.2  | 30  | 30.5 |

Table 5. 3 : ClimGen Results of the statistical tests showing the comparison of the observed precipitation and maximum temperature means and variances with those of 20 year synthetically generated data by ClimGen at Mandura station

|                 | Jan  | Feb  | Mar  | Apr  | May   | Jun   | Jul   | Aug   | Sep   | Oct   | Nov  | Dec  |
|-----------------|------|------|------|------|-------|-------|-------|-------|-------|-------|------|------|
| <b>Rainfall</b> |      |      |      |      |       |       |       |       |       |       |      |      |
| obs.mean        | 2.4  | 1.8  | 22.4 | 31.4 | 138.8 | 307.6 | 530.2 | 529.4 | 312.3 | 125.0 | 3.6  | 1.4  |
| sim. mean       | 3.0  | 2.1  | 20.5 | 27.8 | 137.4 | 303.6 | 549.4 | 503.4 | 338.7 | 111.8 | 4.6  | 2.5  |
| <b>MaxTemp</b>  |      |      |      |      |       |       |       |       |       |       |      |      |
| obs.mean        | 31.6 | 33.1 | 34.6 | 34.7 | 32.2  | 28.6  | 26.6  | 26.3  | 26.6  | 28.3  | 29.8 | 30.9 |
| obs.variance    | 2.6  | 3.1  | 2.6  | 2.9  | 4.3   | 2.8   | 2.9   | 2.2   | 2.5   | 2.0   | 2.4  | 2.6  |
| sim. mean       | 31.6 | 32.7 | 34.6 | 34.7 | 32.4  | 28.7  | 26.6  | 26.5  | 26.5  | 28.3  | 29.8 | 30.7 |

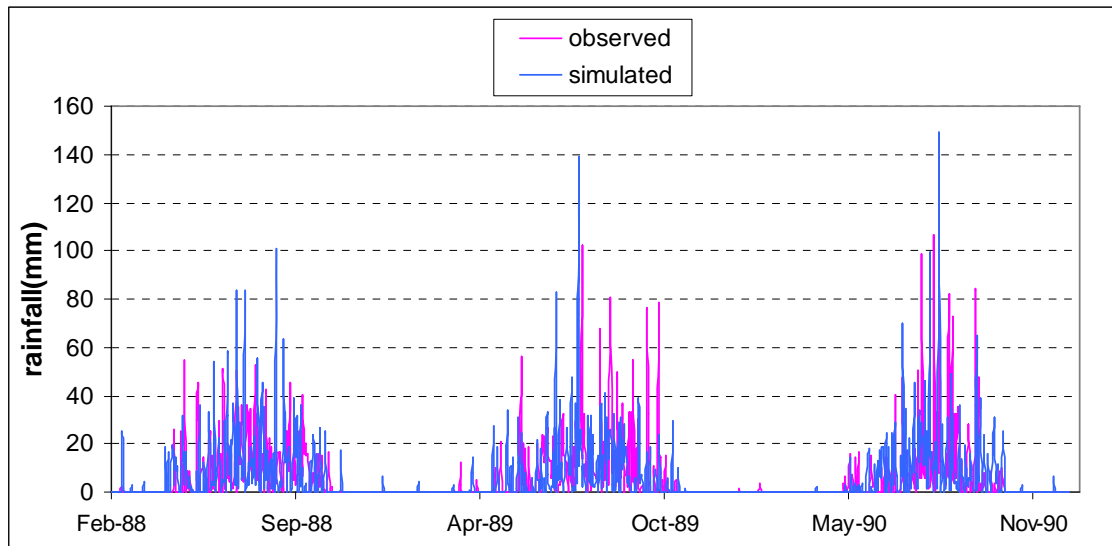


Figure 5. 1 Observed and generated rainfall for Mandura station using ClimGen model

### 5.1.3 Statistical tests

Statistical tests were carried out for annual rainfall and temperature of Bhardar station to check the existence of trend, jump or change points which can be related to past climate change using SPELL-Stat program. Hence the annual rainfall and temperature data series were tested for absence of trend using Spearman's rank correlation test, and stability of variance and mean using Split-record test (F test and t test)

The annual time series of minimum, maximum temperature and annual rainfall of Bhardar station were tested for the absence of trend and it was found that the presence of trend is significant for minimum and maximum temperature where as it is not significant for the annual rainfall. Similarly, F-test for stability of variance and T-test for the stability of the mean were carried out by splitting the data in to six equal non-overlapping years. The results were summarized in Table 5.4. The change point test (Pettit Test) was also carried out to determine the year in which there is a possible change in the data. Probability greater than 0.8 indicates possible change point., Figure 5.3 and 5.4 shows T-test and pettit test result for Bhardar annual rainfall and Table (5.4) shows the possible change point in the F-test and T-test for the same station.

Table 5. 4: Results of F-test and T-test for annual rainfall, max and min temperature of Bhardar stations. X indicates absence of significant change points

| Bhardar station(1961-2002) | Tests for stability of mean and variance |                             |
|----------------------------|--|-----------------------------|
|                            | F-Test                                   | T-test                      |
| Rainfall                   | <b>x</b>                                 | <b>1975,1988,1988</b>       |
| Max Temp                   | 1976,1984                                | 1976,1981,1992              |
| Min Temp                   | <b>1970</b> ,1976,1980,1986,1995         | <b>1971,1973</b> ,1979,1992 |

Except the numbers in bold all the other change points in mean and variance are also supported by Pettitt test (change point test). The maximum temperature change in year 1976 is supported by all tests which mean s we have a good result to conclude about the change. The other change point in min temperature probably has occurred in the year 1979 and 1980 because in addition to the support from Pettit test the closeness of the change point may have implication which may depend on the data quality. There are two time series plots in figure 5.2. The first one shows the annual rainfall data series and the second shows the mean values. As it can be seen from the graph, there are four different mean values with three change points. The mean values before the first, second, third and fourth points are 1553, 1308, 1329 and 1510mm respectively.



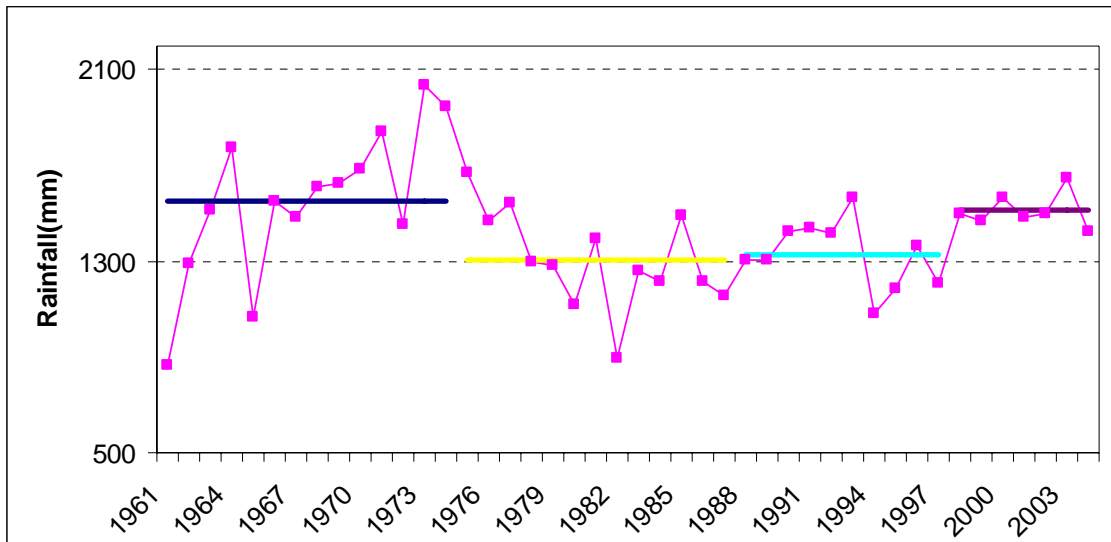


Figure 5. 2: T-test of annual rainfall of Bhardar station

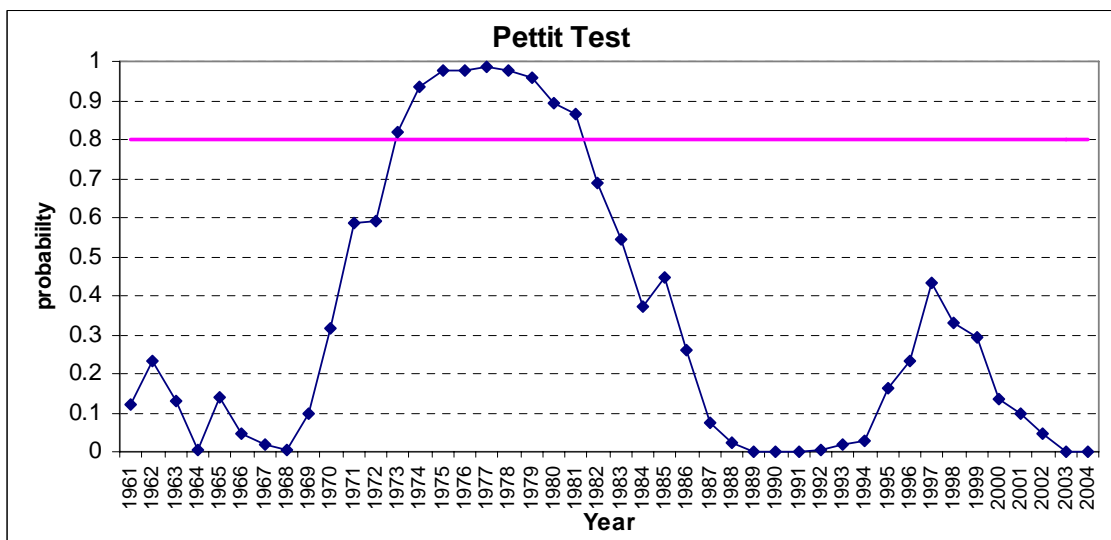


Figure 5. 3 Changing point test of annual rainfall of Bhardar station

From the above discussion we can conclude that there are signals of changes that could be related to climate change. Therefore this study will develop future climate scenarios based on the GCM model outputs to assess the potential climate change impacts on stream flow of Beles. Since GCM model output are not used for impact studies at watershed level, we used downscaling techniques. The results and discussions follows:

## 5.6 Downscaling

Downscaling of daily precipitation was carried out at each selected stations using statistical downscaling model (SDSM) and Time-Lag Recurrent neural network. Minimum and maximum temperature was downscaled at Pawe key station in both cases and the relative change was applied for the other two stations.

### 5.6.1 SDSM

#### 1 Predictor variables selected

Selection of the most relevant predictor variables was carried out through linear correlation analysis and scatter plots (between the predictors and the predictand variables). Observed daily data of large-scale predictor variables representing the current climate conditions (derived from the NCEP reanalysis data sets) was used to investigate the percentage of variance explained by each predictand-predictor pairs. In general, the correlation between the predictor variables and each predictand is very low in case of precipitation as compared with minimum and maximum temperature.

The correlation matrix between predictor variables were used to investigate the association strength between them. Higher value of correlation static's indicates strong association. This correlation is inherent if the p-value returns small ( $p < 0.05$ ) otherwise the correlation may be chance. Therefore in the screening of predictor variables the partial correlation coefficients and p-values were used as selection criteria. Predictor variables that have better spatial and temporal correlation with the predictand at Pawe, Dangila and Bhardar with significance level less than 0.05 were presented in Table 5.5 & 5.6. 500hPa zonal velocity, surface meridional velocity and relative humidity at 500hpa has shown relatively good association with the local precipitation at Pawe, Bhardar, and Dangila respectively once the influence of the other predictors has been removed, where as maximum temperature at Pawe station is strongly correlated with the mean temperature at 2 m, which shows its heavy dependence on regional temperature. On the other hand, minimum temperature at Pawe station is almost equally associated with surface zonal velocity and surface vorticity.

Table 5. 5 List of predictor variables that have better spatial and temporal correlation with the predicatnds at Pawe station with significant level less than 0.05( $p < 0.05$ )

| Predictand      | Predictors (NCEP Reanalysis) | Notations | Partial $r^1$ |
|-----------------|------------------------------|-----------|---------------|
| Precipitation   | Surface vortocity            | P_zaf     | -0.153        |
|                 | 500hpa zonal velocity        | P5_uaf    | -0.17         |
|                 | Relative humidity at 850hpa  | R850af    | +0.036        |
| Max Temperature | Surface air flow strength    | P_faf     | -0.127        |
|                 | 850hpa meridional velocity   | P8_vaf    | +0.149        |
|                 | Mean temperature at 2m       | tempaf    | +0.469        |
| Min Temperature | Surface zonal velocity       | P_uaf     | +0.332        |
|                 | Surface vortocity            | P_zaf     | -0.323        |
|                 | 500hpa geopotential height   | P500af    | +0.234        |

Table 5. 6 :List of predictor variables that have better spatial and temporal correlation with rainfall as predictand ,for Bhardar and Dangila station with significant level less than 0.05( $p < 0.05$ )

| Station | Predictors (NCEP Reanalysis) | Notations | Partial $r^1$ |
|---------|------------------------------|-----------|---------------|
| Bhardar | Surface merodinal velocity   | P_vaf     | -0.124        |
|         | Relative humidity at 850hpa  | r 850af   | +0.103        |
| Dangila | 500hpa zonal velocity        | P5_uaf    | -0.052        |
|         | Relative humidity at 500hpa  | r 500af   | +0.161        |

<sup>1</sup>The partial correlation coefficient( $r$ ) shows the explanatory power that is specific to each predictor.

## 2 Calibration and Validation

From the fifteen years of data representing the current climate condition the first ten years (1987-1996) were considered for calibrating the regression models while the remaining five years of data (1997-2001) were used to validate the model. Some of the SDSM setup parameters for event threshold, bias correction and variance inflation were adjusted during calibration to get the good statistical agreement between observed and simulated climate variables. During the calibration of precipitation downscaling models, in addition to the mean daily precipitation, monthly average dry and wet-spell lengths were used as performance criteria. Figure 5.4 shows the performance of the model during validation for Pawe rainfall and Maximum and minimum temperature, which Table 5.7 shows the statistical performance for all stations

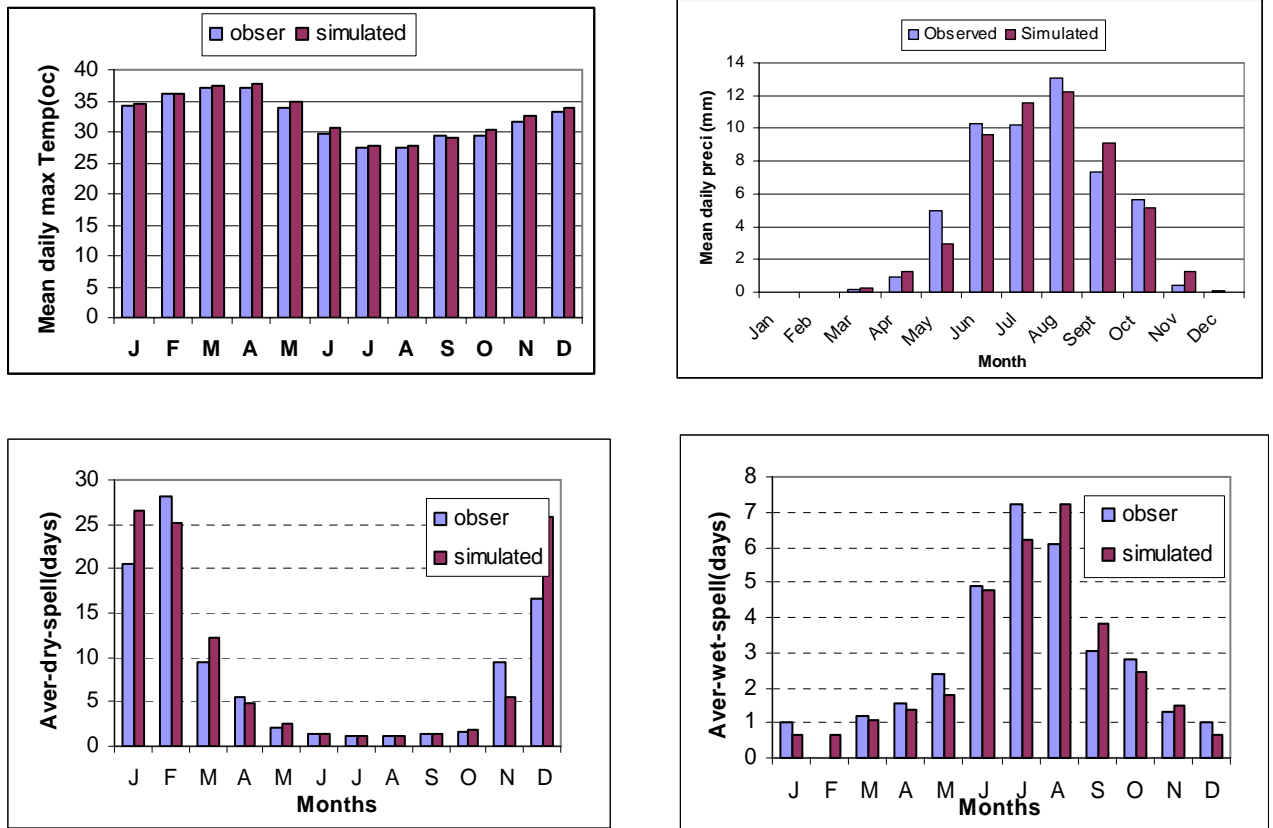


Figure 5. 4: Validation result of SDSM model downscaling of daily precipitation and maximum temperature at Pawe station at Pawe station

Table 5. 7: Model validation statistics with observed data and Large scale Re-analysis data

| Station | predicatnd | RMSE | MAE   | obs.std | Sim.std | Obs.mean | sim.mean | Correlation |
|---------|------------|------|-------|---------|---------|----------|----------|-------------|
| Pawe    | Tmax       | 1.82 | 1.34  | 3.76    | 3.63    | 32.2     | 32.7     | 0.89        |
|         | Tmin       | 1.9  | 1.438 | 2.97    | 2.74    | 16.5     | 16.4     | 0.78        |
|         | Rainfall   | 10.1 | 5.1   | 10.83   | 5.4     | 4.5      | 4.48     | 0.39        |
| Dangila | Rainfall   | 7.74 | 4.33  | 8.64    | 5.11    | 4.68     | 4.64     | 0.46        |
| Bhardar | Rainfall   | 8.7  | 4.13  | 9.57    | 5.01    | 3.95     | 3.95     | 0.43        |

The observed and simulated mean daily max temp shows good agreement (Figure 5.5). The higher correlation coefficients Table 5.7 shows the same information. Mean daily precipitation shows underestimation in the months March, and July, overestimation during the months February, April and September and well agreement is seen for the rest. The average dry spell length plot also shows overestimation in the month of January and December. In general precipitation is identified by many researchers as one of the most problematic variable in downscaling. As discussed before, precipitation is a conditional process; it is dependent on other intermediate process like occurrence of humidity, cloud cover, and /or wet-days.

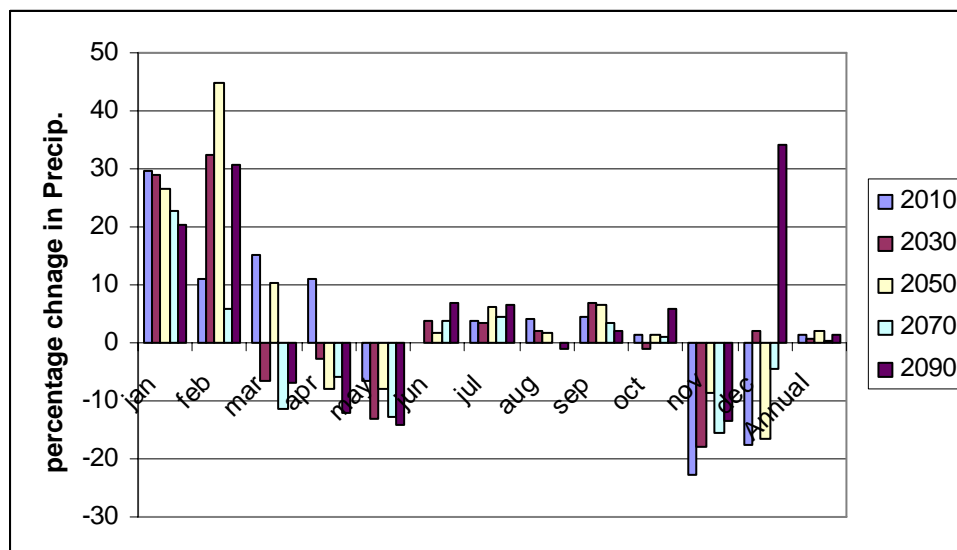
### 3 Scenario generation

After the downscaling model has been setup and validated, the next step is to use this model to downscale the future climate change scenario simulated by GCM. This means large scale predictor variables to be used as input to downscaling model as they are derived from GCM simulation output.

Twenty ensembles of synthetic daily time series were generated for two SERS emission scenarios (A2 and B2) for the period of 139 years (2061-2099) and the ensemble mean of the twenty ensemble members were used for impact analysis using Hydrological model for this case HEC-HMS. Downscaling of rainfall and temperature were done for six periods namely, the current (base period) (1987-2001), the 2010(2002-2019), the 2030s (2020-2039), the 2050s (2040-2059), the 2070s (2060-2079) and the 2090s (2080-2099) using the calibrated model

Global scale models are usually concerned with long-term average conditions. For example a model developed for average conditions in January doesn't mean that a particular January in the period for which a climate model prediction is made will have these conditions, only that the conditions apply to an average January(Henderson-Sellers and J.Robison, 1986). That is why we are considering the long-term-average in each data period.

#### Rainfall



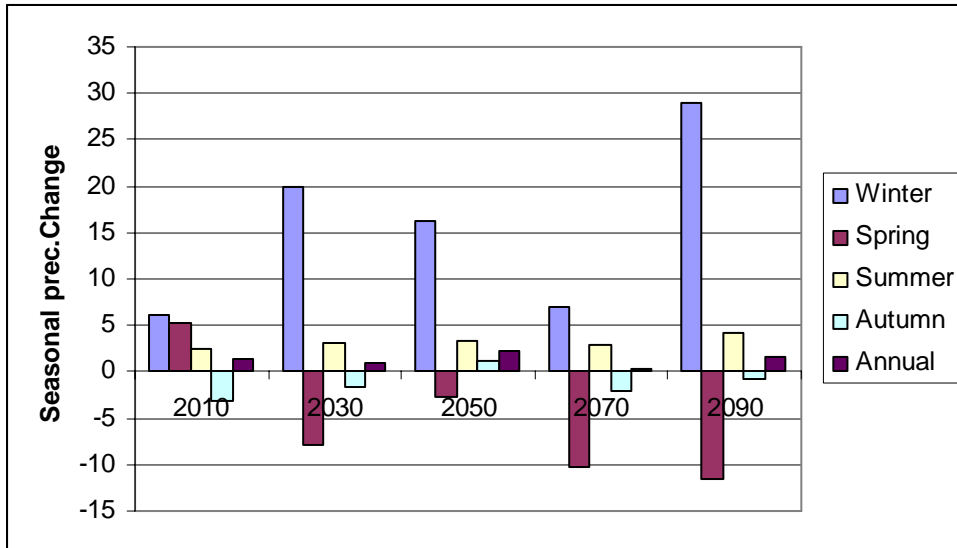


Figure 5. 5 : Pawe rainfall increase/ decrease in percentage for A2scenrio

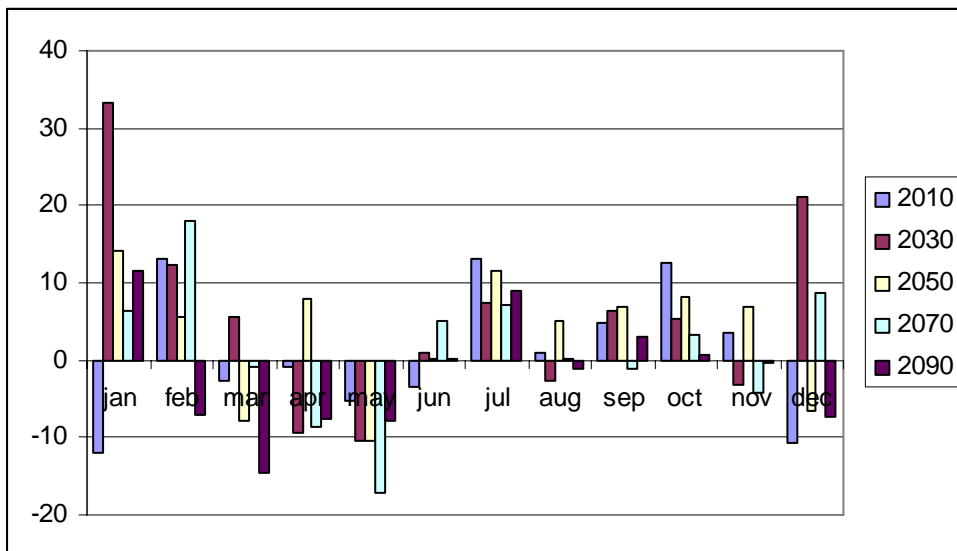


Figure 5. 6: Pawe rainfall increase/ decrease in percentage for B2scenrio

As it can be seen in figures 5.5 and 5.6 precipitation increase would be expected during rain season (Kirmet) where as spring precipitation shows a decrease for both scenarios. Precipitation is also expected to increase in winter. But these changes are not as pronounced as we can see from the figures, because the absolute precipitation values are small in winter. For example in 2090s in the month of December precipitation change from 0.05mm/month to 0.06 mm/month shows 34 % precipitation increases.

## Max Temperature

As it can be seen in (Figures 5.7 &5.8), the maximum temperature shows an increasing trend for both scenarios. In general the maximum temperature change is very significant in the rainy seasons, kiremt. The maximum increment of +2.7 °c for A2 scenario and +1.7°C B2 scenario in 2090s in the month of July. In general the annual max temp change between the current climate condition and 2090s will be about 1.2 °C for A2 scenario and 0.75 °C for B2 scenario.

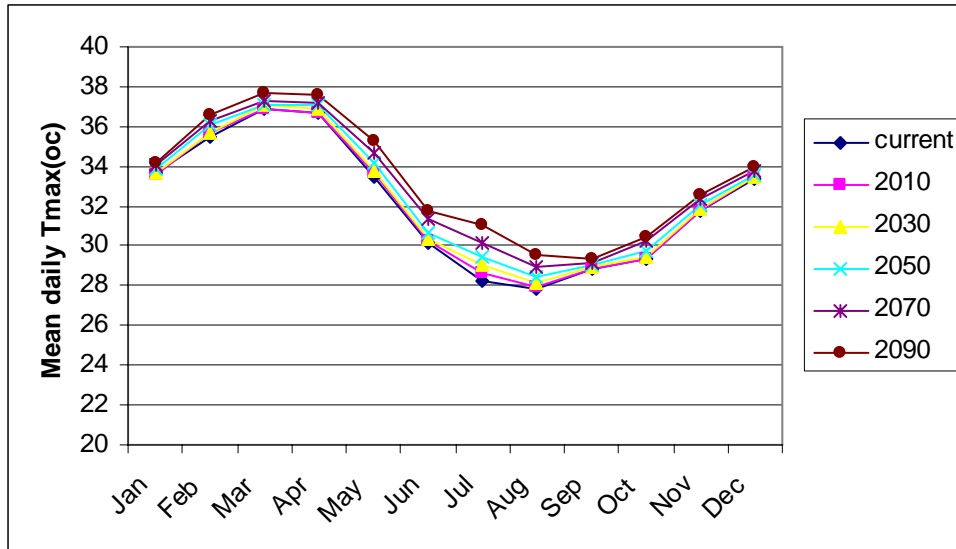


Figure 5. 7: General trend in maximum temperature corresponding to A2a scenario

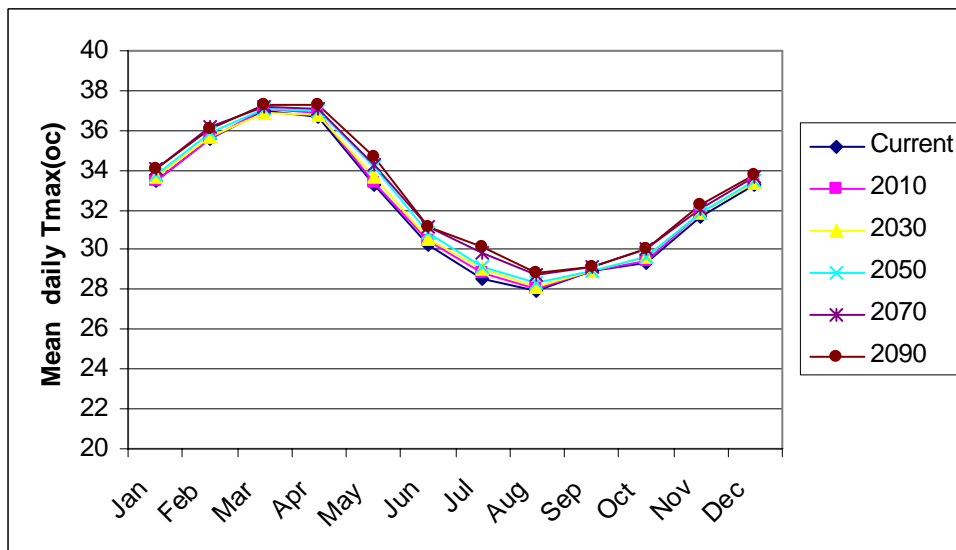


Figure 5. 8: General trend in maximum temperature corresponding to B2a scenario

## Minimum Temperature

Like the maximum temperature there is a general increasing trend minimum temperature for both A2a and B2a scenarios (Figures 5.9 & 5.10). The annual increase in minimum temperature from the current climate condition for 2090s will be +1.7oc for A2a scenario and + 1.2 oc for B2a scenario

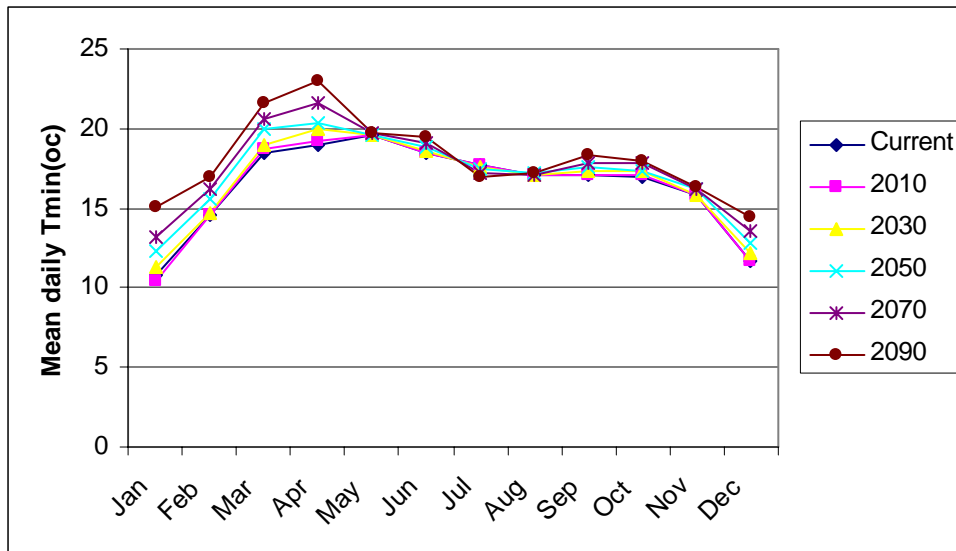


Figure 5. 9 : General trend in minimum temperature corresponding to A2a scenario

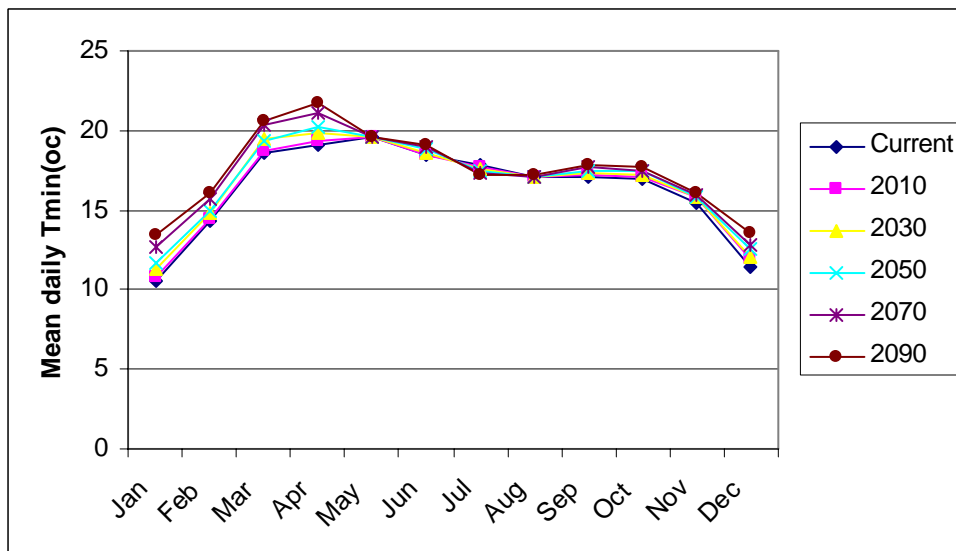


Figure 5. 10: General trend in minimum temperature corresponding to B2a scenario



In 2090s max increase is observed in the month of January (+4.4 oc) and a decrease in the month of July (-0.8oc) for A2a scenario. And B2a scenario shows an increase of +2.9oc and decrease (-0.5 oc) for the same period from the current condition.

### 5.6.2 Time Lagged Feed forward Neural networks (TLFN)

The neural network model for this study area is developed using Neuro-Solutions neural network development environment. From the fifteen years of observed data (1987-2001) the first ten years were used for training and the rest as testing. The twenty six predictor variables derived from the NCEP reanalysis dataset were used as input to the neural network model while daily precipitation amount and maximum and minimum temperatures were specified as desired output and modeled separately. First with the twenty six predictor variables as input the model is trained and sensitivity analysis was done to determine the most relevant predictors which need to be used in further retraining. Then neural network was retained with few selected predictor variables till acceptable validation performance is achieved. Hyperbolic tangent activation function is used at both the hidden and output layers of the neural networks and for learning the DeltaBarDelta was selected. The number of hidden nodes was optimized and nine neurons in the hidden layer gave good result for Pawe rainfall downscaling where as for Dangila five neurons in the hidden layer were found to be the optimal.

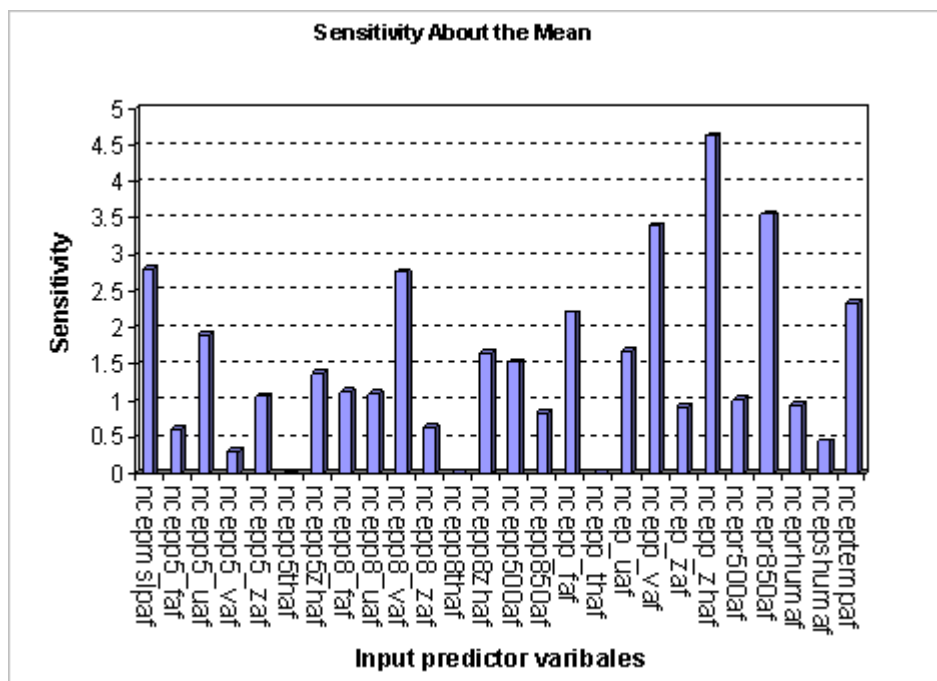


Figure 5. 11: Sensitivity of a TLFN (in downscaling precipitation at Pawe stations) to each of the predictors variables used as input to the network.

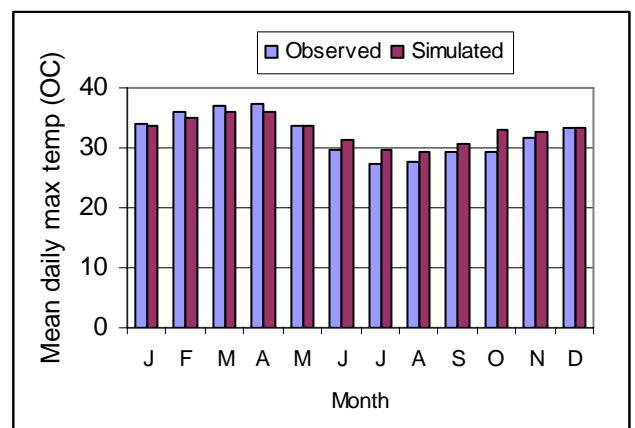
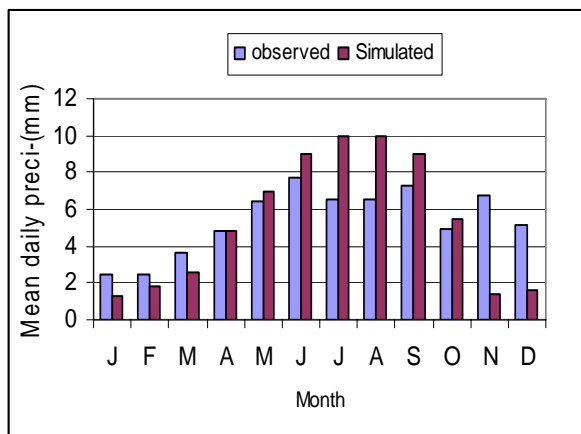
Similar to the sensitivity analyses of rainfall at Pawe station (Figure 5.12), the sensitivity analysis were carried out for maximum and minimum temperature at Pawe station as well as for precipitation at Dangila station and the potential predictors are summarized in Table 5.8

Table 5. 8: sensitive predictor variables

| Potential Predictor variables | Pawe |      |      | Dangila |
|-------------------------------|------|------|------|---------|
|                               | RF   | MaxT | MinT | RF      |
| Mean sea level pressure       | X    | X    |      |         |
| 500 hpa zonal velocity        | X    | X    |      | X       |
| 850 hpa meridional velocity   | X    |      |      |         |
| Surface air flow strength     | X    | X    |      | X       |
| Surface meridional velocity   | X    |      |      | X       |
| Surface divergence            | X    | X    |      | X       |
| Relative humidity at 850 hpa  | X    | X    | X    | X       |
| Mean temperature at 2 m       | X    | X    | X    | X       |
| 500 hpa geopotential height   |      | X    |      |         |
| Surface specific humidity     |      | X    | X    |         |
| 850 hpa zonal velocity        |      |      | X    | X       |
| 850 hpa vorticity             |      |      | X    |         |
| 850 hpa divergence            |      |      | X    |         |
| Surface vorticity             |      |      | X    | X       |
| Relative humidity at 500 hpa  |      |      | X    |         |

Table 5. 9 Model validation statistics

| Station | Predictand          | RMSE | Correlation |
|---------|---------------------|------|-------------|
| Pawe    | Maximum Temperature | 2    | 0.86        |
|         | Minimum Temperature | 1.8  | 0.8         |
|         | Rainfall            | 10.3 | 0.4         |



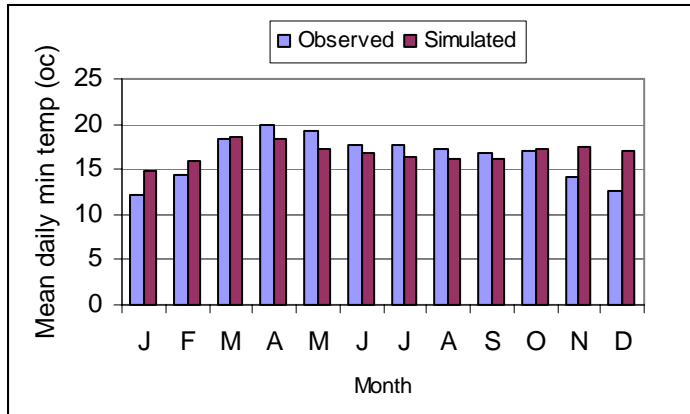


Figure 5. 12 Validation results of TLFN downscaling daily rainfall, maximum and minimum temperature at Pawe station

As it can be seen in figure 5.12 the validation result for mean daily rainfall shows an overestimation for the months of June, July, August and September and underestimation in the months of November and December. In general the validation results show good agreement for the case of maximum and minimum temperature.

Figure 5.13 and 5.14 show s the mean daily maximum and minimum temperature for the current and future climate scenarios. As it can be seen in Figure 5.13 the maximum temperature increase is higher in the summer seasons. The annual maximum temperature shows an increase of 2.2 °c in 2090s from the current condition. Figure 5.16 shows the mean daily minimum temperature for the current condition and future climate scenario. The minimum temperature increase is higher in winter and spring. The annual minimum temperature shows an increase of 2.75 °c in 2090s from the current condition. The monthly minimum temperature increase also varies from 1.78°c in the month of July to 3.6 °c in the month of January in the same period.

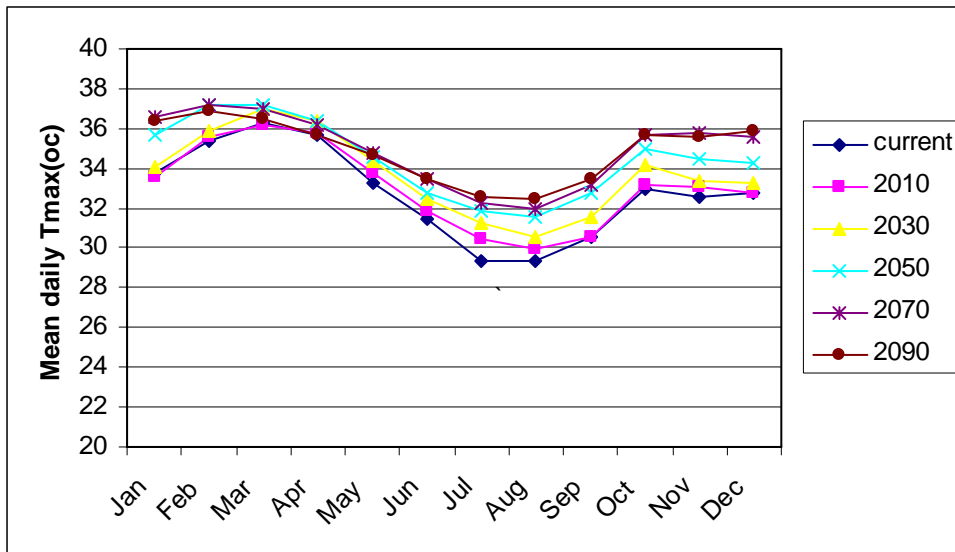


Figure 5. 13: General trend in max temperature corresponding to A2a scenario

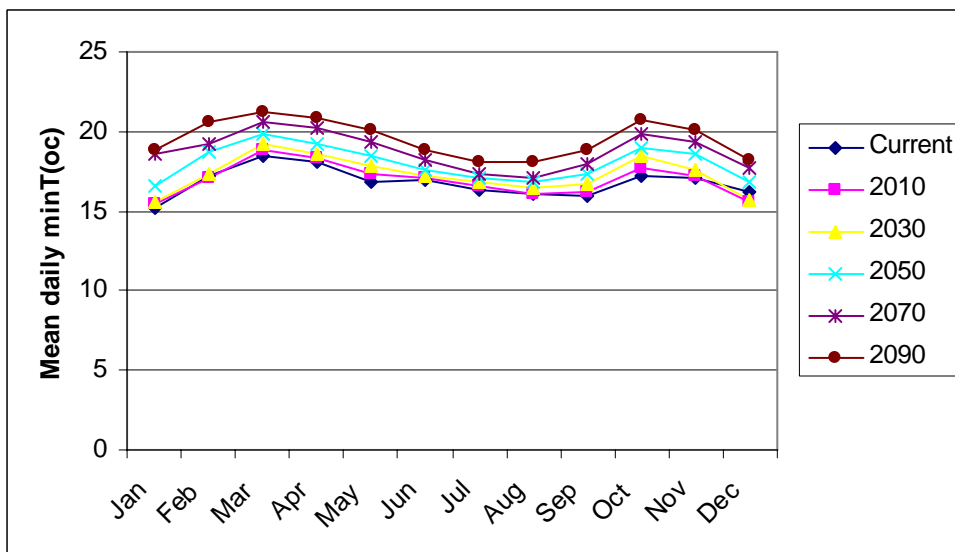


Figure 5. 14: General trend in min temperature corresponding to A2a scenario

## 5.7 HEC-HMS Hydrological Model Results

### 5.7.1 Calibration

HMS has the capabilities to process automated calibration in order to minimize a specific objective function, such as sum of the absolute error, sum of the squared error, percent error in peak, and peak-weighted root mean square error. However in this case, the resulted automated parameters are not reasonable and practical. Therefore manual calibration method was adopted to determine a practical range of the parameter values preserving the hydrograph shape, minimum error in peak discharges and volumes but since the output is determined by the inputs, the weather generated rainfall imposed a lot of effort on the calibration. Therefore to assist the calibration process additional stochastic calibration was used.

As discussed in the previous sections the flow records of Main Beles has similar gap as observed in the meteorological stations. Therefore because of the limited data available flow calibration was carried out using five year of data 1994-1998

The whole 12 parameters needed for the SMA were taken into consideration in this simulation. The maximum infiltration rate and the maximum soil depth as well as the percolation rates and groundwater components had significant influence on the simulated flow discharges. The remaining parameters were adjusted to match the simulated and observed peak flows, volumes and hydrograph shape. Table 5.10 shows the optimal parameters found in calibration. Due to the influence of the synthetically generated weather parameters such as rainfall and temperature the flow simulated by the model and the observed flow data was difficult to match in time (stochastic nature of the input parameters (Figure 5.15)). The coefficient of determination ( $R^2$ ) during calibration was found to be 0.55 (Figure 16). The stochastic nature of precipitation effect on the simulated hydrograph was handled by stochastic calibration. In the stochastic calibration observed and simulated discharge time series were arranged in descending order and the objective function,  $\sum (Q_{obs} - Q_{sim})^2$  was minimized by observing the plot of observed and simulated discharge. As it can be seen in (Figure, 17) the observed and simulated hydrograph coincides very well. Although the model was less efficient during deterministic calibrations, its performance is well acceptable during stochastic calibration. Therefore we can conclude that the model can reasonably be used for the intended purpose.

Table 5. 10 Optimal model calibration parameters

| Routhing parmeters                   |      |
|--------------------------------------|------|
| Muskingum k(HR)                      | 6    |
| Muskingum x                          | 0.1  |
| Loss parmeters                       |      |
| Canopy storage (mm)                  | 1.3  |
| Surface storage(mm)                  | 12   |
| Max Infiltration(mm/hr)              | 1.9  |
| Soil storage (mm)                    | 200  |
| Tension storage (mm)                 | 150  |
| Soil percolation (mm/hr)             | 0.9  |
| Ground water 1 storage(mm)           | 50   |
| Ground water 1 percolation (mm/hr)   | 0.6  |
| Ground water1 coefficient (hr)       | 600  |
| Ground water 2 storage (mm)          | 80   |
| Ground water 2 percolation (mm/hr)   | 0.6  |
| Ground water 2 coefficient(hr)       | 1800 |
| Transform                            |      |
| Storage coefficient(hr)              | 60   |
| Time of concentration (hr)(sub-1 &2) | 12   |
| Time of concentration (hr)(sub-3)    | 24   |

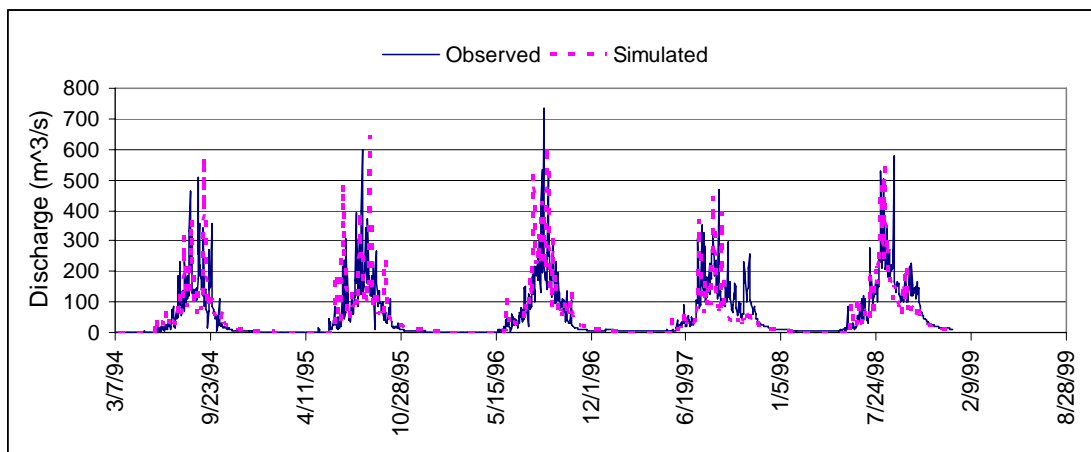


Figure 5. 15 Simulated and observed flow hydrographs

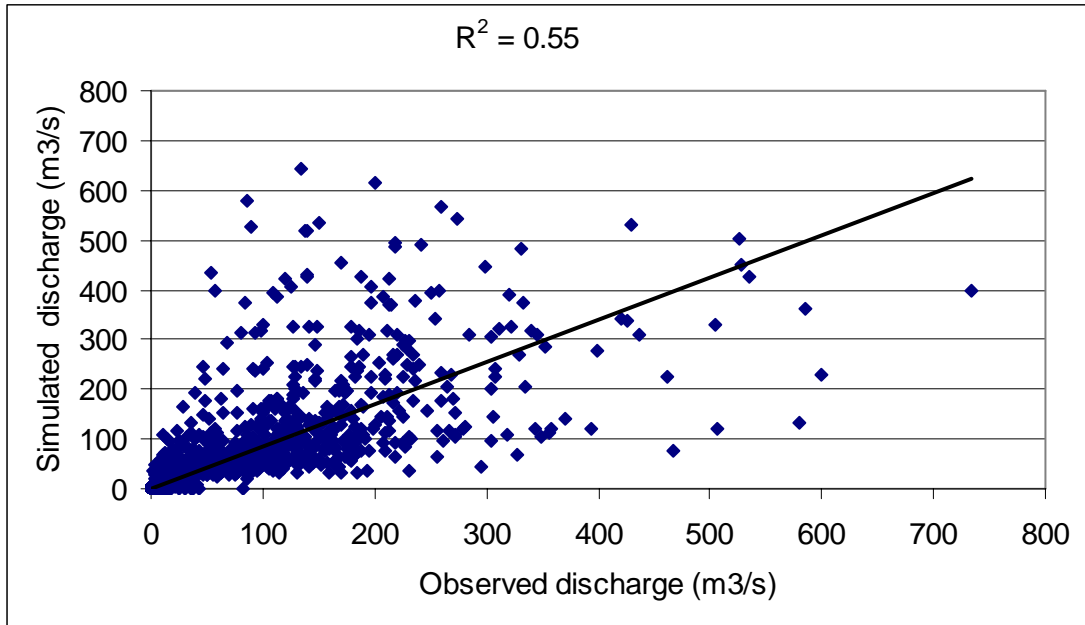


Figure 5. 16 Observed vs. simulated (calibration)

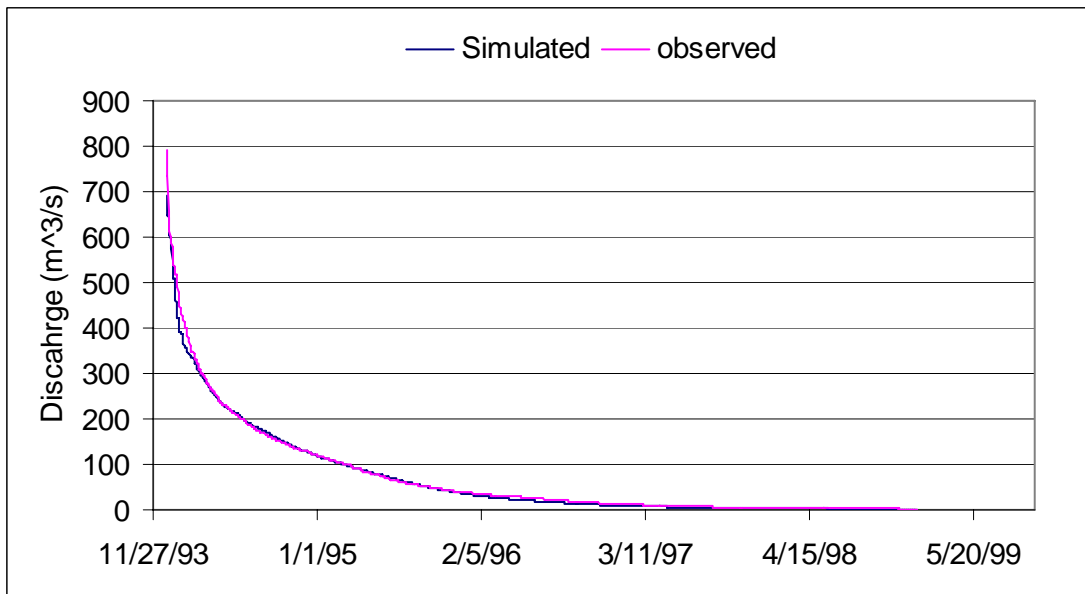


Figure 5. 17: Simulated and observed flow in model calibration (stochastic calibration)

### 5.7.2 Validation

Model validation was carried out over the period of 1999-2001. As it can be seen in (Figure 5.18) the model performance is improved, the coefficient of determination in this case is found to be 0.6 (Figure 5.19). The observed and simulated flow hydrograph show well agreement except in peak flow in year 1999. In general the model performed reasonably in simulating flows for periods outside of the calibration period, based on adjusted parameters during calibration.

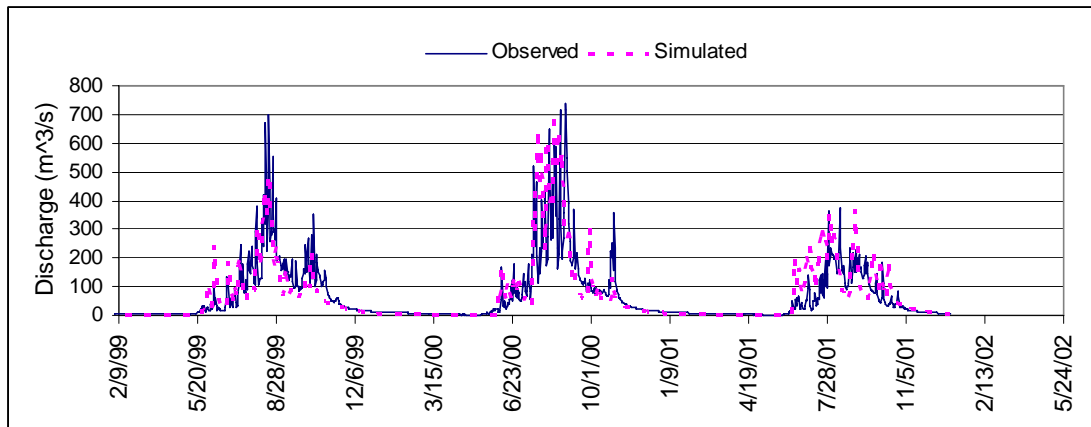


Figure 5. 18 : Simulated and observed flow hydrographs

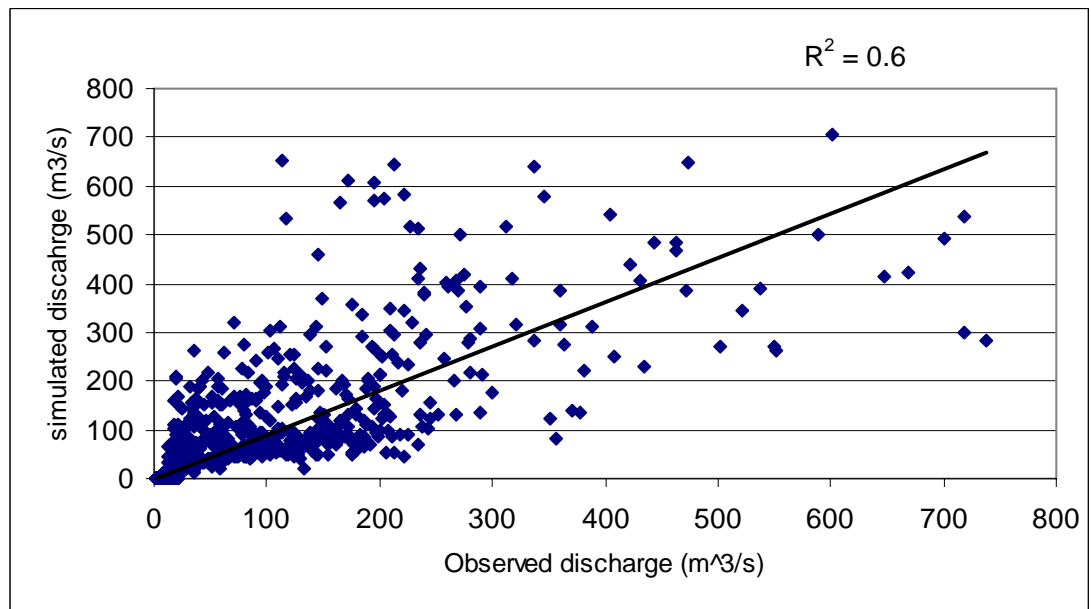
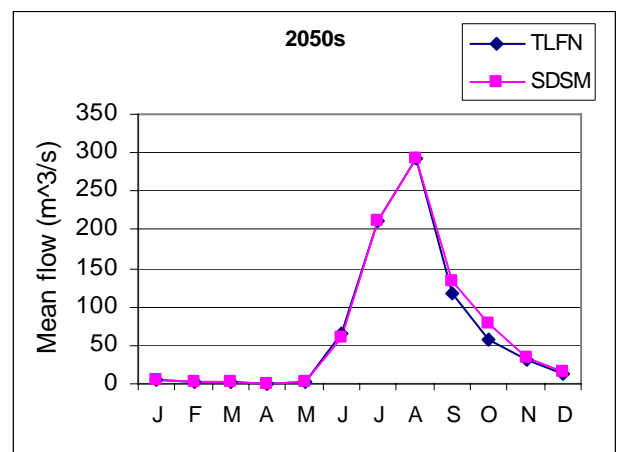
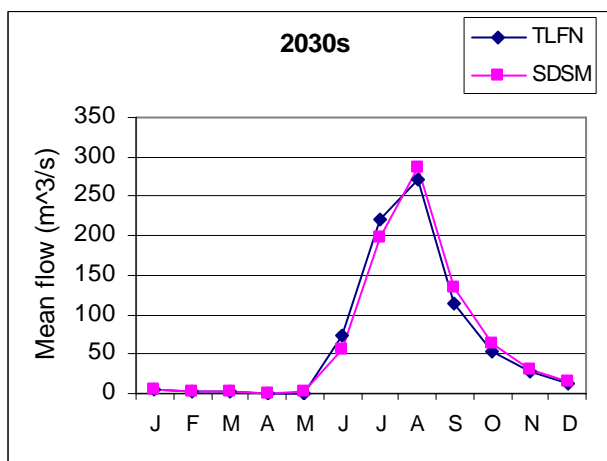
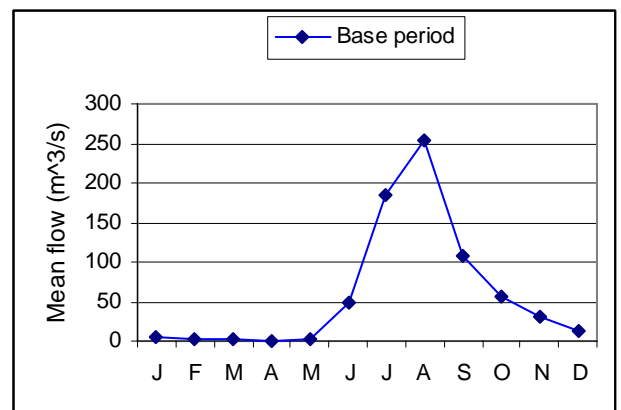
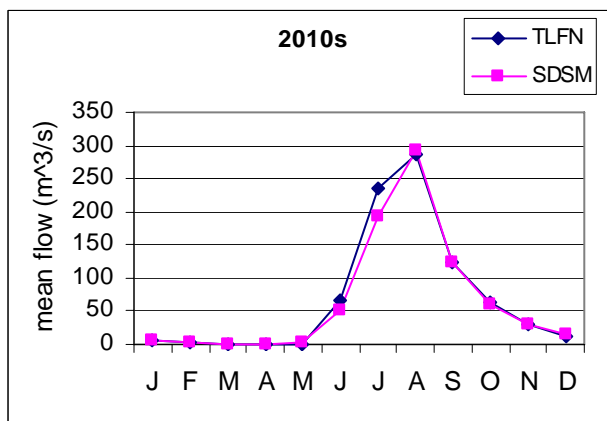


Figure 5. 19 observed vs. simulated (validation)



### 5.7.3 Model simulation corresponding to future climate change scenarios

After calibrating the hydrological model the next step is simulation of flows corresponding to future climate conditions by using the downscaled precipitation and temperature data for each emission scenarios discussed in the previous sections. This will help to identify any specific trend in the mean flows in the Main Beles River corresponding to future time horizon considered in this study. The future simulation is done with the downscaled precipitation and temperature data from both SDSM and TLFN. The downscaled precipitation data were divided in to six data period and the hydrologic model is re-run for each case. One of the main limitations of this study is that, except temperature and rainfall all the other climate variables such as wind speed, sunshine hours, and relative humidity were assumed to be constant which is not possible in actual case. Since climate is a complex process and it involves many complex feedbacks this assumption doesn't hold but the main objective of this study is to provide an indicative possible effect of climate change on the stream flow assuming changes only in the two main drivers (Temperature and precipitation).



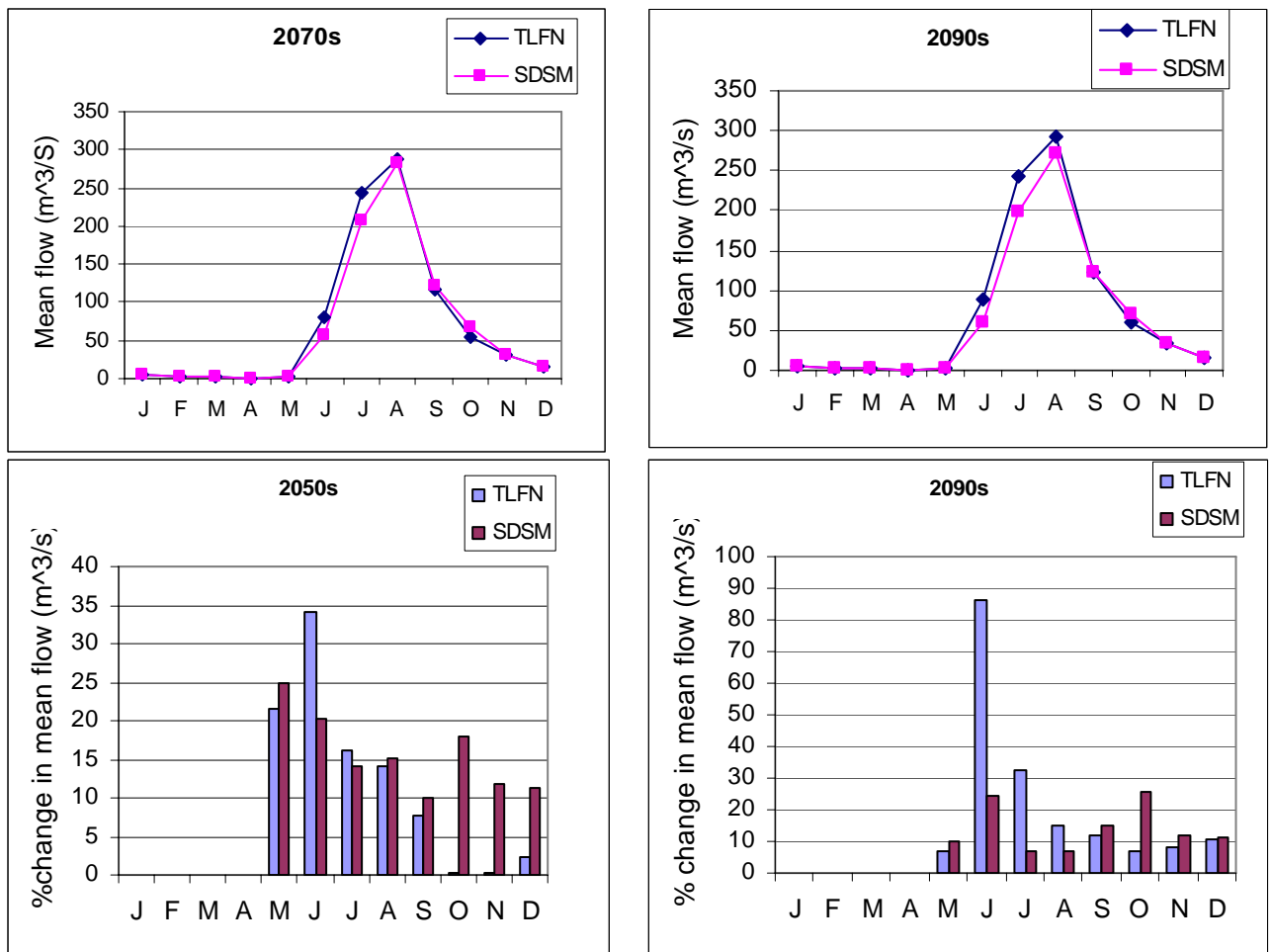


Figure 5. 20: Comparison of average mean monthly and percentage flow change –A2a scenario

Fig 5.20 shows the average monthly mean flow and the average percentage change in mean flow. As it can be seen in the plots the two downscaling techniques simulate reasonably well the stream flow except the very large percentage change observed in the month of June for the case of TLFN for both 2050s and 2090s. Also there is big difference in the winter flow in 2050s. In general the simulated mean flow with the two methods shows an increase in rainy season flows. SDSM downscaling data resulted in an increase in mean annual flow by 18.5% during the period between the current and the 2050s and TLFN downscaled data shows an increase in mean flow by 12.8 % during the same period , where as in 2090s SDSM shows an increase of 11% and TLFN shows 22.6%.

Downscaling for B2a scenarios was carried out only using SDSM model. Therefore this section presents, the simulation results of stream flow change based on the SDSM downscaled precipitation and temperature inputs.

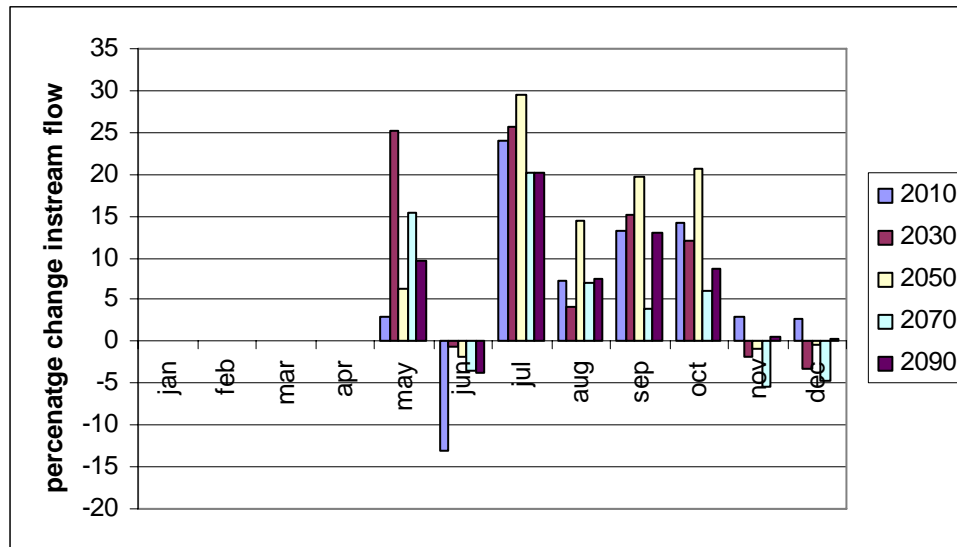


Figure 5. 21: Percentage change in stream flow for B2a scenario

As it can be seen in (Figure 5.21) the stream flow shows general increase except for June for all periods and December and November for 2070s and 2090s. The June flow under scenarios A2a shows large increase but on the other hand here it shows decreasing (13%). This difference could be possible since the increase/decrease of stream flow is determined by the relative increase/decrease of precipitation and temperature which act in opposite direction: Such differences have been reported earlier in similar studies. One reason may be uncertainties in emission scenarios.

## 5.8 Crop water requirements

The crop water requirements analysis for future development of irrigation in the Upper Beles area under climate change scenario was carried out using CROPWAT model. Two cropping period (complementary and supplemental irrigation periods) were used for the analysis. The principal crops grown in the area were identified from the local information during filed visit and literature. According to Tefferra et al (1992) the principal crops grown in the area by the local population are finger millet, teff, sorghum and maize and minor crops include chickpea, sesame and chillies. Among the cereals, finger millet account 32 %, teff 21%, sorghum 15 % and maize 12 % of the total crop area.

Mater plan studies (USBR, 1964) also described the anticipated cropping pattern during irrigation and non-irrigation seasons in the Upper Beles project area. The cropping pattern projection made was based on crops which are well accepted in the

Ethiopian diet and are required for industrial uses or for export, but which are well adapted to sub tropical climate. They also reported that cereal grains, pulses, oilseeds, cotton, peppers and tobacco offer good possibilities in the area. Corn, millet, sorghum, peas, lentils, sesame and peppers well grow during the irrigation seasons and have wide domestic demand. For the non irrigated or rainy season which extends roughly from June to October, corn, millet, chick peas and sesame were projected as suitable crops.

Therefore the cropping pattern as well as suitable crops during the two irrigation periods was defined based on previous studies in the area. The cropping patterns adopted in this study are: maize 40 %, sesame 15 %, sorghum 20 %, Millet 15 % and peppers 10 % for irrigation period and for supplemental period, maize 60 % Millet 20 % and sesame 20 %. The planting date for the irrigation period and supplemental periods were assumed to be October 1 and April respectively although in reality all crops can not be planted as the same date.

The crop irrigation requirements were computed for the two seasons on decadal basis and the maximum values are summarized in Table 5.11. In each case 10 hour daily irrigation and application efficiency of 65 % were assumed.

Table 5. 11 Summary of Irrigation water requirements for the two irrigation seasons

| Month                                 | base period | 2010 | 2030 | 2050 | 2070 | 2090 |
|---------------------------------------|-------------|------|------|------|------|------|
| Irrigation water requirements(l/s/ha) |             |      |      |      |      |      |
| October                               | 0.43        | 0.43 | 0.46 | 0.43 | 0.48 | 0.43 |
| November                              | 1.75        | 1.75 | 1.75 | 1.78 | 1.78 | 1.80 |
| December                              | 1.85        | 1.85 | 1.87 | 1.90 | 1.92 | 1.89 |
| January                               | 1.90        | 1.90 | 1.90 | 1.92 | 1.92 | 1.95 |
| February                              | 0.46        | 0.46 | 0.46 | 0.46 | 0.46 | 0.46 |
| April                                 | 0.55        | 0.48 | 0.53 | 0.46 | 0.58 | 0.62 |
| May                                   | 0.26        | 0.29 | 0.34 | 0.31 | 0.34 | 0.33 |
| Eto(mm/period)                        | 1571        | 1575 | 1582 | 1591 | 1601 | 1615 |
| CWR(Etm)                              | 874         | 876  | 880  | 886  | 891  | 899  |
| Total RF(mm/period)                   | 1067        | 1089 | 1080 | 1110 | 1083 | 1105 |

As it can be seen in Table 5.11 the crop water requirement change from the current condition is insignificant:-The reason is that the potential evapotranspiration calculated by Penman formula doesn't show significant change. Penman formula is more sensitive to humidity change. In this study we have made an assumption that the other variables will remain constant, which may not be true. Therefore since the increase in temperature will directly relate with solar radiation, duration of sunshine hour and other variables, assuming these variables as constant will not enable us to identify the impact of temperature increase on the potential evapotranspiration. This case was also checked with sensitivity as follows: Keeping rainfall variation constant

we have increased temperature by 1 °c and 2 °c, and the result is this increase doesn't bring significant change. In conclusion the crop water requirement even though is not significant, it shows a positive slope. Which means, if we add the variability of other climatic factors, the crop water requirement may be corrected to increase

## 5.9 Synthetic scenarios

As reviewed in the previous chapter 3 (section 3.4) Synthetic scenarios (Incremental scenario) are one of the scenarios that are commonly used in impact studies. These scenarios are based on techniques where particular climatic (or related) elements are changed by realistic but arbitrary amount (e.g. +1, 2, 3, 4 °c from the baseline temperature and ±5, 10, 15 and 20% change from the baseline precipitation. They are commonly applied to study the sensitivity of an exposure unit to a wide range of variations in climate, often according to a qualitative interpretation of projections of future regional climate from climate model simulations (IPCC-TGCI, 1999). For example (Tarekegn, 2005) employed this method to study impacts of Climate Change on Water Resources of Lake Tana Sub-Basin Using WatBal Model and (Hailemariam, 1999) also used this method to study the impact of climate change on water resource of Awash River basin in Ethiopia. These scenarios will not be outdated by changes in GCM output and facilitate intuitive understanding of impacts by water resource managers and policy makers.

In this study we have applied a hypothetical increase in temperature (+2 °c) and change in rainfall (-20,-10, +10 or +20%). Sensitivity analysis based on this scenario as it can be seen in Table 5.12 showed that a drier and warmer climate change scenario results in reduced runoff. A 20% decrease in rainfall coupled with a 2 °c increase in temperature would result in 42% decrease in annual runoff.

Table 5. 12: stream flow change under synthetic scenario

| Climate scenario | May   | Jun   | Jul   | Aug   | Sep   | Oct   | Nov   | Dec   | Annual |
|------------------|-------|-------|-------|-------|-------|-------|-------|-------|--------|
| T+2;P -20%       | -46.5 | -67.2 | -56.4 | -39.8 | -39.7 | -13.6 | -15.3 | -14.0 | -41.87 |
| T+2;P -10%       | -29.9 | -44.0 | -27.6 | -19.8 | -20.8 | -7.4  | -7.4  | -6.8  | -21.62 |
| T+2;10%          | 39.0  | 51.1  | 27.3  | 19.8  | 23.0  | 8.3   | 6.9   | 6.3   | 22.40  |
| T+2;20%          | 92.6  | 109.7 | 53.6  | 39.5  | 48.3  | 20.2  | 12.8  | 11.8  | 45.64  |



## **6 Benefit of the study for the Nile Basin Initiative**

Population growth, economic development and climate change has proven to be the cause of the rising water demand. In particular Climate change on water resources are becoming an emerging concerns to decision-makers. The alteration of climate in a region drives the change in the hydrological regime and thus produces stream flow variability

In the past, water resource planning and management relied on the assumption that the future climate would be the same as the past. And most water resources policies and programs were developed under these assumptions(Gleick, 1997). The traditional way of water resource management is reported to be inadequate. Therefore, long-term planning taking into account climate variability and change is increasingly important. Furthermore, water resource planning must accommodate the various, and often conflicting, demands for water. Nile River is one of International River increasingly facing the frequent variability of runoff in upstream basins: thus making water resources management of downstream countries difficult (Kim, 2007). It has been found that most regions within the Nile Basin are sensitive to climate change (Conway, 2004). To date limited research is carried out on climate change on Upper Blue Nile. Almost all the studies were focused on the impact of climate change on the whole basin and very little research has been carried out on the climate change impact assessment of the Tana sub-basin. Beles sub-basin is one of the major tributary of Upper Blue Nile River. The water resource potential of this basin is so far not well assessed in particular with respect to climate change

Therefore this study has been carried out in Beles sub-basin. The study results as well as the experience gained will contribute to the NBI objectives in the following ways: First this study was carried out under limited data. Data is one of the limiting factors in any development studies. This study has used weather generator model that can suit for limited data based on comparative study. This knowledge and experience gained will help to carry out similar studies in other sub-basins which has similar data problem. Secondly the knowledge and experience gained in downscaling global climate model output is highly beneficial for the basin. It is widely recognized that the current available GCM models, runs at coarser resolutions and their direct output can not be used for impact assessments. This study adopted two methods of downscaling. This would have significant advantage in addressing the climate change impact studies over the basin.

Thirdly, model integration: In this study we have used series of models; Weather generator models, downscaling models, hydrologic model and CropWat model. Therefore this will also help to carryout studies in the basin in an integrated way.

Fourthly, impact assessment: Analysis of the temporal variations in stream flow due to climate variability can help water resources planners and decision makers in assessing the impact of climate change on irrigation, and get insight upon which appropriate decisions about agricultural development can be made. In addition to climate change data obtained from Global Circulation Models (GCM), impact assessments were carried out based on a range of “what if”(synthetic) scenarios. These scenarios facilitate intuitive understanding of impacts by water resource managers and policy makers. In general the study will benefit NBI in many ways. The experience and knowledge gained during the study is also very valuable.



## 7 Conclusions and Recommendations

### 7.1 Conclusions

The two weather generator models used in this study mainly differ in the choice of the daily distribution used. ClimGen use Weibull distribution for precipitation generation where as LARS-WG uses semi-empirical distribution. In conclusion ClimGen has showed a good performance indicating representative weather data of rainfall and temperature can be generated with limited data. The model's ability to work on limited data will make it suit for data sparse area like Beles basin, but further investigation with more spatially distributed stations needs to be performed. The two models were equally good in generating temperature series. In general this conclusion doesn't reflect that LARS-WG model is less efficient in weather generation. LARS-WG performance has been compared with the most widely used weather generator model WGN and it has showed very good performance((Semenov *et al.*, 1998a)). LARS-WG has wide application in downscaling GCM outputs to mention few (Dibike and Coulibaly, 2005; Khan *et al.*, 2005; Semenov and Barrow, 1997)

The stream flow change corresponding to the downscaled precipitation and temperature by the two methods shows that SDSM estimates an increase in mean annual flow by 18.5% during the period between the current and the 2050s and TLFN shows an increase in mean flow by 12.8 % during the same period, where as in 2090s SDSM shows an increase of 11% and TLFN 22.6%, the two models don't lead to one conclusion.. There are two major factors that may be the reason for the difference. The first is the input data supplied for each model. The TLFN model used data gaps and missing data filled by the ClimGen weather generation model, where as SDSM used the actual observed data by tagging the missing data in the way that the model can recognize it. The second main reason for the difference in the downscaling results can be attributed to the respective modeling techniques of the two models. For instance in SDSM, the downscaling method is a multiple regression model between sensitive large scale predictor variables and local scale predictand. This relationship is further improved by adjusting means and variance of downscaled data by using bias correction and variance inflation so that the model can generate outputs closer to the observed data. Moreover SDSM considers daily precipitation downscaling as a conditional process, in which precipitation amount are conditioned on the occurrence of wet/dry days. On the other hand ANN exhibits some noticeable shortcomings as compared to SDSM The ANN model does not consider precipitation downscaling as a conditional process; rather it establishes a direct nonlinear relationship between large-scale predictors and local scale predictand without considering the precipitation occurring process, which causes significant errors in downscaled daily precipitation. Moreover, the ANN model is deterministic, restricting to create only one time series

where as due to its hybrid nature SDSM model not only considers deterministic relationship between predictors and predictand but also refine this relationship by using variance inflation in the model to account for the relationship of the input and outputs unexplained by deterministic model and produces many ensemble outputs.

In conclusion, due to the above reasons the stream flow change based on the SDSM downscaling results should be considered for further impact assessments. However the downscaling in this study is made using only one GCM model output (HadCM3). Previous studies showed that data taken from different GCMs could differ significantly. Therefore care should be taken in interpreting the results for further impacts assessments.

The hydrological model (HEC-HMS) calibrated and validated for the Upper Beles basin shows that the model is less skilful in explaining the hydrological process. Two main reasons can be mentioned: accuracy of the rainfall input and lack of practical range of physical parameters in the soil moisture accounting model.

In conclusion, although the model returns low coefficients of determination due to the above reasons the model is well calibrated using the stochastic calibration. The volume error is kept to minimum; the low values of r-square are the results of the unmatched timing in the peaks. In general without much detailed information of the physical processes in the basin it was possible to calibrate the model reasonably well.

In this study, the hydrological model parameters were assumed to remain valid under changing climatic conditions, and the same sets used both for current and future simulations. However, these assumptions may not be held in the future under changing land use and hydrological processes.

## 7.2 Recommendations

Based on the findings and limitations noted in this study the following recommendations were drawn.

- Further research should consider different GCM model output, downscaling techniques and emission scenarios in order to minimize the uncertainties associated with each model. Downscaling methods such as the application of regional climate models that have already been applied to the Nile Basin should be further applied in large river basin like, Beles.
- Since the main source of water for the Tana Beles Hydropower and Upper Beles Irrigation project is Lake Tana, continuing research should consider the impact of climate change on the Lake Tana.
- This study is believed to give an insight about the likely impact of climate change at the watershed level. Therefore future studies should be continued in different parts of the Ethiopian basins.
- Future research should also include adaptation options to climate change.
- Although the increase in runoff has positive implication for the proposed Dangur Hydropower project at the middle of the basin, inclusion of climate change impact is sought to be advantages from future flood risks.
- Results of any impact studies are highly dependent on the quality of input data; therefore increasing the number of meteorological and hydrological stations is very important. In addition the data handling system and quality check should be improved.



## References

- Allen, R. G., Pereira, L. S., Raes, D., and Smith, M. (1990) *FAO Irrigation and Drainage Paper, NO.56, Crop Evapotranspiration (guidelines for computing crop water requirements)*.
- Conway, D. (2004) From head tributaries to international river: Observing and adapting to climate variability and change in the Nile basin. *Global Environmental Change*.
- Coulibaly, P., and Dibike, Y. B. (2004) Downscaling of Global Climate Model Outputs for Flood Frequency Analysis in the Saguenay River System. *Final Project Report prepared for the Canadian Climate Change Action Fund, Environment Canada, Hamilton, Ontario, Canada*.
- Dahmen, E. R., and Hall, M. J. (1990) *Screening of Hydrologic Data: Tests for Stationarity and Relative Consistency*, International Institute for Land Reclamation and Improvement/ILRI(49), The Netherlands.
- Deboch, W.-S. A. (2002) *Gumuz and Highland Resettlers : Differing Strategies of Livelihood and ethnic relations in Metekel, North western Ethiopia*, PhD thesis, university of Gottingen.
- Dibike, Y. B., and Coulibaly, P. (2005) Hydrologic impact of climate change in the Saguenay watershed: comparison of downscaling methods and hydrologic models. *Journal of Hydrology (Amsterdam)*, **307**(1/4), 145-163.
- Dibike, Y. B., and Coulibaly, P. (2006) Temporal neural networks for downscaling climate variability and extremes. *Neural Networks*.
- Fowler, H. J., Blenkinsop, S., and Tebaldi, C. (2007) Linking climate change modelling to impacts studies: recent advances in downscaling techniques for hydrological modelling. *International journal of climatology*.
- Geathun, Y. G. E. (2007) *Constructing a homogeneous Rainfall dataset to study Climate of Ethiopia*, The University of Reading.
- Gleick, P. H. (1997) Water Planning and Management under climate change. *Journal of the American Water Works Association*.
- Gragne, A. S. (2007) *Catchment Modeling and Preliminary Application of Isotopes for Model Validation in Upper Blue Nile Basin , Lake Tana, Ethiopia*, UNESCO-IHE.
- Guzman, A., and Librada, M. (2004) SPEL-Stat, A time series Statistical analysis program.
- Hailemariam, K. (1999) Impact of Climate Change on the Water Resources of Awash River Basin Ethiopia. *CLIMATE Research*
- HEC (2006a) *HEC-DSSVue, HEC Data Storage System Visual Utility Engine, user's Manual*.
- HEC (2006b) *Hydrological Modeling system (HEC-HMS) User's Manual , US Army corps of Engineers*
- Henderson-Sellers, A., and J. Robison, P. (1986) *Contemporary Climatology*, Longman Singapore.
- Hessami, M., Gachon, P., ourda, T. B. M. J., and St-Hilaire, A. (2007) Automated regression-based statistical downscaling tool. *Environmental Modeling and Software , Science Direct*.
- Houghton, J. (2004) *Global Warming, The Complete Briefing*, Third Edition.

- IPCC-TGCI (1999) *Guidelines on the use of Scenario Data for Impact and Adaptation Assessment*.
- IPCC (2001) *Climate Change 2001: The scientific basis, Contribution of Working Group I to the Third Assessment report of the Intergovernmental Panel on Climate Change* [ J.T. Houghton, Y. Ding, D.J. Griggs, M. Noguer, P.J. van der Linden, X. Dai, K. Maskell and C.A. Johnson (eds.)]. , Cambridge University Press,Cambridge.
- IPCC (2007) *Climate Change 2007: The Physical Science Basis. Contribution of Working Group I to the Fourth Assessment Report of the Intergovernmental Panel on Climate Change* [Solomon, S., D. Qin, M. Manning, Z. Chen, M. Marquis, K.B. Averyt, M.Tignor and H.L. Miller (eds.)] Cambridge University Press, Cambridge, United Kingdom and New York, NY, USA
- Khan, M. S., Paulin Coulibaly, and Dibike, Y. (2005) Uncertainty analysis of statistical downscaling methods. *Journal of hydrology*.
- Kim, U. (2007) *Regional Impacts of Climate Change on Water Resources of the Upper Blue Nile River Basin, Ethiopia*, Utah State University.
- Lijalem, Z. A. (2006) *Climate Change Impact on Lake Ziway Watershed Water Availability,Ethiopia*, University of Applied Sciences Cologne,Germany.
- Miller, K. A., and Yates, D. (2004) *Climate Change and Water Resources*. National Center for Atmospheric Reserach.
- Mohammed, Y. A., denHurk, B. J. J. M. V., H.H.G.Savenije, and W.G.M.Bastiaansen (2005) Hydroclimatology of the Nile: results from a regional climate model. *Hydro.Earth Syst.Sci*.
- Muluye, G. Y., and Coulibaly, P. (2007) Seasonal reservoir inflow forecasting with low-frequency climatic indices: a comparison of data-driven methods. *Journal of Hydrology Special issue: Hydroinformatics*.
- O'Hare, G., Sweeney, j., and Wilby, R. (2005) Weather, Climate and Climate Change: Human Perspectives. 403.
- Richard Jones, Maria Noguer, David Hassell, Debbie Hudson, Simon Wilson, Geoff enkins, and Mitchell, J. (2004) *Generating high resolution Climate Change Scenarios using PRECIS*.
- SaliniCostruttori (1989) *Tana Beles Project ETHIOPIA*.
- Semenov, M. A., and Barrow, E. M. (1997) Use of A stocatsic Weather Generator in the Development of Climate Change Scenarios. *Climate change*.
- Semenov, M. A., Brooks, R. J., Barrow, E. M., and Richardson, C. W. (1998a) Comparison of the the WGEN and LARS-WG stochastic weather generators for diverse climates  
*Climate Research Clim Res*.
- Semenov, M. A., J.Brooks, R., Barrow, E. M., and W.Richardson, C. (1998b) Comaprison of the WGEN and LARS-WG stochastic weather generators for diverse climate. *Climate Research Clim Res*.
- SMEC (2008) *Hydrological study of the Tana-Beles sub-basins*
- Tarekegn, D. (2005) Impacts of Climate Change on Water Resources of Lake Tana Sub-Basin Using WatBal Model

- Tefferra, M., T/Berehas, w., kebede, T., and Molla, G. (1992) *The Transitional Government of Ethiopia office of Prime Minister Economic Sector, Status of the Tana-Beles project (Achievements, problems and proposals)*.
- Tingem, M., Rivington, M., Azam-Ali, S., and Colls, J. (2007) Assessment of the ClimGen stochastic weather generator at Cameroon sites. *African journal of Environmental Science and Technology*.
- USBR (1964) *Land and Water Resources of the Blue Nile Basin Appendix VI - Agricultural and Economics*.
- Wilby, R., Charles, S., Zorita, E., Timbl, B., Whetton, P., and Means, L. (2004) *Guidelines for use of Climate Scenarios Developed from Statistical Downscaling Methods*.
- Wilby, R. L., and Dawson, C. W. (2007) *SDSM 4.2 — A decision support tool for the assessment of regional climate change impacts, User Manual*
- Wilby, R. L., and Harris, I. (2006) A framework for assessing uncertainties in climate change impacts: Low-flow scenarios for the River Thames, UK. *WATER RESOURCES RESEARCH*.
- Wilby, R. L., and Wigley, T. M. L. (1999) Precipitation Predictors for Downscaling: Observed and General Circulation Model Relationships. *INTERNATIONAL JOURNAL OF CLIMATOLOGY*.
- Wilby, R. L., Wigley, T. M. L., Conway, D., P.D.Jones, B.C.Hewitson, Main, J., and Wilks, D. S. (1998) Statistical downscaling of general circulation model output A comparison of methods. *WATER RESOURCES RESEARCH*.



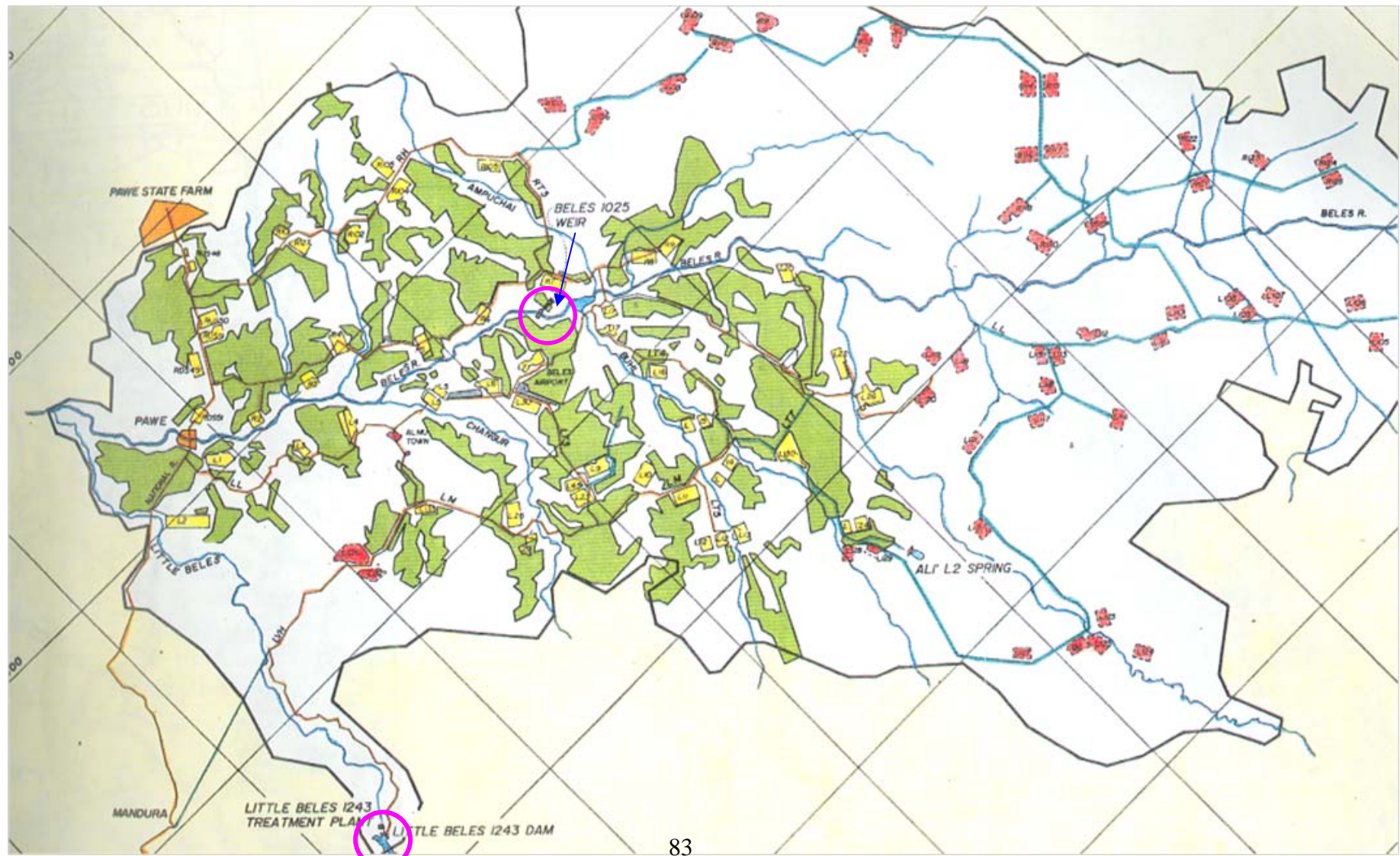


# **ANNEXES**

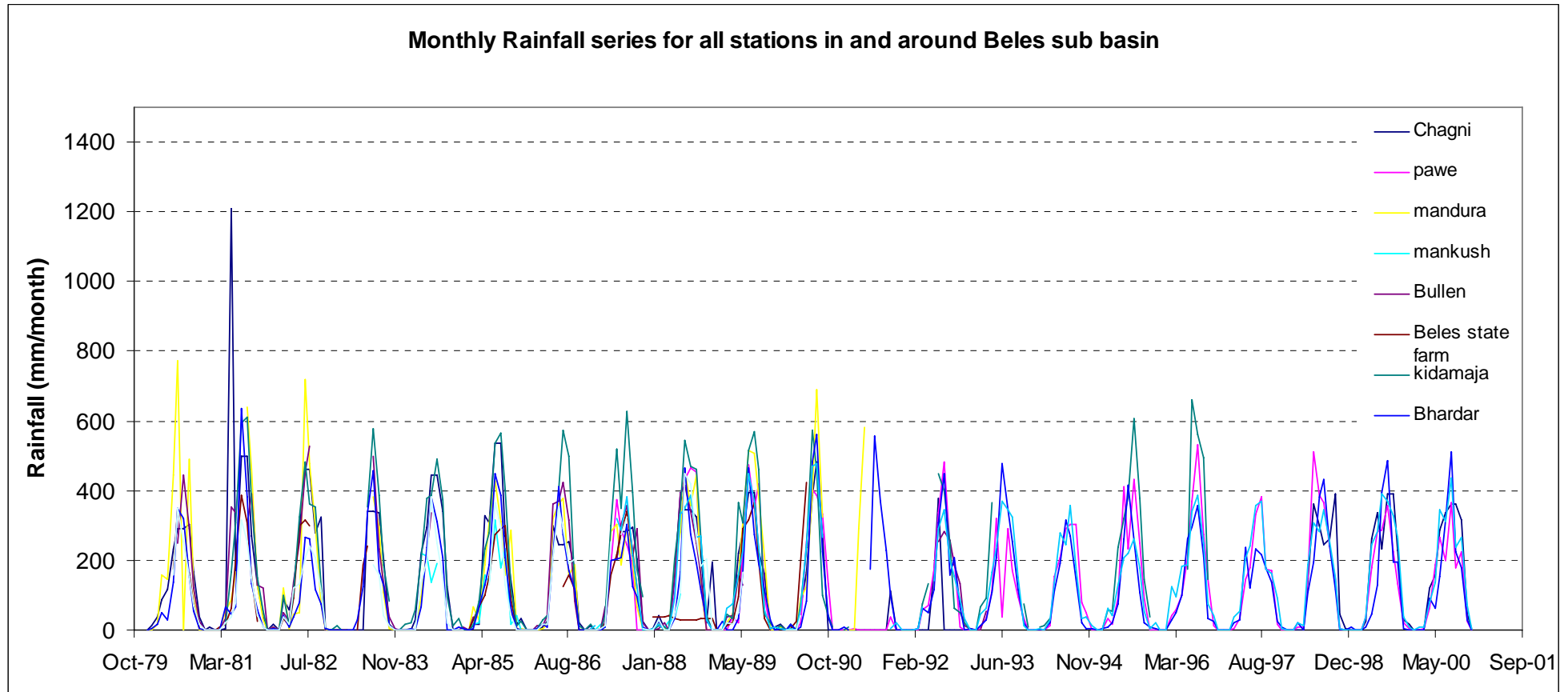
Annex A: Monthly Rainfall data of Kunzila station

|      | STATION:- | KUNZILA |      | REGION:- | GOJAM | Monthly Rainfall(mm) |       |       |       |       |       |
|------|-----------|---------|------|----------|-------|----------------------|-------|-------|-------|-------|-------|
|      | JAN       | FEB     | MAR  | APR      | MAY   | JUN                  | JUL   | AUG   | SEP   | OCT   | NOV   |
| 1980 | x         | x       | x    | x        | x     | 159.1                | 347.8 | 253.8 | 154.7 | 68.8  | 16.3  |
| 1981 | 0.0       | 0.0     | 0.0  | 20.0     | 36.5  | 77.3                 | 317.0 | 254.3 | 151.1 | 43.4  | 8.5   |
| 1982 | 0.0       | 0.0     | 38.6 | 17.1     | 121.8 | 132.9                | 206.6 | 240.2 | 207.6 | 112.1 | 7.6   |
| 1983 | x         | x       | x    | x        | x     | x                    | x     | 187.5 | 158.4 | 40.7  | 10.5  |
| 1984 | 0.0       | 0.0     | 0.0  | 0.0      | 137.3 | 198.3                | 381.5 | 249.7 | 151.3 | 19.5  | 0.0   |
| 1985 | 0.0       | x       | x    | x        |       | 130.5                | 365.1 | 294.1 | 130.0 | 43.1  | 0.0   |
| 1986 | 0.0       | 0.0     | 0.0  | 17.4     | 17.3  | 206.0                | 353.8 | 289.2 | 191.9 | 201.9 | x     |
| 1987 | 0.0       | 0.0     | 2.3  | 11.8     | 252.3 | x                    | 273.3 | 322.3 | x     | x     | 4.3   |
| 1988 | 0.0       | 30.5    | 0.0  | 0.0      | 43.4  | 113.0                | 448.6 | 419.0 | 263.2 | 182.2 | 202.6 |
| 1989 | 0.0       | 0.0     | 21.3 | 17.4     | 48.2  | 166.1                | x     | x     | x     | x     |       |
| 1990 | x         | 0.0     | 0.0  | 0.0      | 43.5  | x                    | x     | 244.5 | x     | x     | x     |

Anne B: Tana-Beles Project Site Map (adopted from Tana Beles Project



Annex-C: Monthly Rainfall series in and around Beles Sub basin (1980/81 -1999/2000)



Annex-D: Daily Flow record time series of Main Beles River at Bridge

